

LOEWNER CHAINS.

Michel BAUER and Denis BERNARD

Service de Physique Théorique de Saclay *,
CEA-Saclay, 91191 Gif-sur-Yvette, France
 michel.bauer@cea.fr, dbernard@spht.saclay.cea.fr

Abstract These lecture notes on 2D growth processes are divided in two parts. The first part is a non-technical introduction to stochastic Loewner evolutions (SLEs). Their relationship with 2D critical interfaces is illustrated using numerical simulations. Schramm's argument mapping conformally invariant interfaces to SLEs is explained. The second part is a more detailed introduction to the mathematically challenging problems of 2D growth processes such as Laplacian growth, diffusion limited aggregation (DLA), etc. Their description in terms of dynamical conformal maps, with discrete or continuous time evolution, is recalled. We end with a conjecture based on possible dendritic anomalies which, if true, would imply that the Hele-Shaw problem and DLA are in different universality classes.

Growth phenomena are ubiquitous in the physical world at many scales, from crystals to plants to dunes and larger. They can be studied in many frameworks, deterministic or probabilistic, in discrete or continuous space and time. Understanding growth is usually a very difficult task. This is true even in two dimensions, the case we concentrate on in these notes.

Yet two dimensions is a highly favorable situation because it allows to make use of the power of complex analysis in one variable. In many interesting cases, the growing object in two dimensions can be seen as a domain, i.e. a contractible open subset of the Riemann sphere (the complex plane with a point at infinity added). A deep theorem of Riemann asserts that such a domain, whatever complicated and fancy, is conformally equivalent to a simple reference domain, which is usually taken as the upper-half plane or the unit disk. This conformal equiva-

*CEA/DSM/SPHT, Unité de recherche associée au CNRS, URA 2306 du CNRS

lence is unique once an appropriate normalization, which may depend on the growth problem at hand, has been chosen. Cauchy's theorem allows to write down an integral representation for the conformal map as an integral along the boundary of the reference domain, involving a density. This density is time dependent. Then the time derivative of the conformal map has an analogous representation and a nice way to specify the growth rule is often directly on this density. This leads to the concept of Loewner chains, which is the central theme of these notes. We shall illustrate Loewner chains in several situations.

Our aim is to give a pedagogical introduction to a beautiful subject. We wanted to show that it leads to many basic mathematical structures whose appearance in the growth context is not so easy to foresee, like Brownian motion, integrable systems and anomalies to mention just a few. We have also tried to stress that some growth processes have rules which are easy to simulate on the computer. A few minutes of CPU are enough to get an idea of the shape of the growing patterns, to be convinced that something interesting and non trivial is going on, and even sometimes to get an idea of fractal dimensions. This is of course not to be compared with serious large scale simulations, but it is a good illustration of the big contrast between simple rules, complex patterns and involved mathematical structures. However, other growth models, and among those some have been conjectured to be equivalent to simple ones, have resisted until recently to precise numerical calculations due to instabilities.

To avoid any confusion, let us stress that being able to describe a growth process using tools from complex analysis and conformal geometry does not mean that the growth process itself is conformally invariant at all. Conformal invariance of the growth process itself puts rather drastic conditions on the density that appears in the Loewner chain.

This is illustrated by the first part of these notes, which deals with conformally invariant interfaces and their relation to stochastic Loewner evolutions. This part is an elaboration of the the main points developed during the lectures.

The second part is an introduction to a larger class of processes describing the growth of possibly random fractal planar domains and a review of some of their basic properties. Due to lack of time, this part was not presented during the lectures.

The study of the continuum limit of non-intersecting curves on the lattice has been a subject of lasting interest both in mathematics and in physics. A famous example is given by self-avoiding random walks. The motivation comes from combinatorics, but also from statistical mechan-

ics. Two dimensions is most interesting because a non-intersecting curve is the boundary between two domains and can very often be interpreted as an interface separating two coexisting phases.

At a critical point and for short range interactions, such interfaces are expected to be conformally invariant. The argument for that was given two decades ago in the seminal paper on conformal field theory [1]. The rough idea is the following. At a critical point, a system becomes scale invariant. If the interactions on the lattice are short range, the model is described in the continuum limit by a local field theory and scale invariance implies that the stress tensor is traceless. In two dimensions this is enough to ensure that the theory transforms simply –no dynamics is involved, only pure kinematics– when the domain where it is defined is changed by a conformal transformation.

The local fields are classified by representations of the infinite dimensional Virasoro algebra and this dictates the way correlation functions transform. This has led to a tremendous accumulation of exact results using conformal field theory (CFT). A situation that is well under control is that of unitary minimal models. The Hilbert space of the system splits as a finite sum of representations of the Virasoro algebra, each associated to a (local) primary field, and the corresponding correlation functions can be described rather explicitly. The study of non-local objects like interfaces at criticality has not seen such a systematic development and only isolated though highly artful results [2, 3, 12] have been discovered using conformal field theory techniques.

Non local objects like interfaces are not classified by representations of the Virasoro algebra but the reasoning that led O. Schramm to the crucial breakthrough [4], i.e. the definition of stochastic Loewner evolutions (SLEs), rests on a fairly obvious but cleverly exploited statement of what conformal invariance means for an interface. Surprisingly it allows to turn this problem into growth problem, something which looks natural only a posteriori. For some years, probabilistic techniques have been applied to interfaces, leading to a systematic understanding that was lacking on the CFT side. A sample, surely biased by our ignorance, can be found in refs.[5, 6, 7, 8, 9]. There is now a satisfactory understanding of interfaces in the continuum limit. However, from a mathematical viewpoint, giving proofs that a discrete interface on the lattice has a conformally invariant limit remains a hard challenge and only a handful of cases has been settled up to now.

There is now a good explanation of the –initially mysterious– relationship between SLE and CFT. This was one of the main topics of the lectures. Though this aspect is mostly due to the work of the present

authors ([10], but see also [11]), we have decided to be very sketchy. The interested reader is referred to the literature.

Stochastic Loewner evolution is a simple but particularly interesting example of growth process for which the growth is local and continuous so that the resulting set is a curve without branching. Of course other examples have been studied in connection with 2d physical systems. The motivations are sometimes very practical. For instance, is it efficient to put a pump in the center of oil film at the surface of the ocean to fight against pollution? The answer has to do with the Laplacian growth or Hele-Shaw problem [14]. The names diffusion limited aggregation [15], see Figure (1.1), and dielectric breakdown [16] speak for themselves. Various models have been invented, sometimes with less physical motivation, but in order to find more manageable growth processes. These include various models of iterated conformal maps [17], etc. See refs.[18] for recent reviews. As mentioned before, in most cases the shape of the growing domains is encoded in a uniformizing conformal map whose evolution describes the evolution of the domain. The dynamics can be either discrete or continuous in time, it can be either deterministic or stochastic. But the growth process is always described by a simple generalization of the Loewner equation called a Loewner chain.

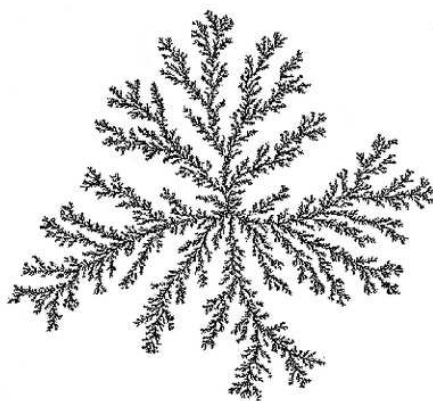


Figure 1.1 An example of DLA cluster obtained by iterating conformal maps.

The general understanding of these Loewner chains is still embryonic, in strong contrast with the case of Loewner evolutions, which deal with local growth. For many problems the most basic question are unanswered. For instance, as we shall explain below, Laplacian growth is at

the same time a completely integrable system and an ill-posed problem because it develops singularities in finite time. Hydrodynamics gives a natural regularization via the introduction of surface tension. It has been argued for some time that in the limit of vanishing surface tension one retrieves a model which is in the same universality class as diffusion limited aggregation. But the experimental and numerical evidence is inconclusive and there is no consensus. In fact, at the end of these notes we shall give an argument suggesting that they belong to different universality classes. This is very conjectural, but as should be clear from this introduction, non-local growth processes are certainly a source of interesting and challenging problems.

Table of contents:

- Section 1: Critical interfaces and stochastic processes.
- Section 2: Loewner chains.

1. CRITICAL INTERFACES AND STOCHASTIC PROCESSES

The following pedagogical introduction to conformally invariant random curves breaks in two part. The first is a list of examples of critical interfaces on the lattice and some of their properties. The second is a presentation of O. Schramm’s derivation of SLE.

In this part the upper-half plane is used as a reference geometry.

1.1 THREE EXAMPLES AND A GENERALITY

Let us start with three examples. Our aim is to explain their definitions, to show a few samples and, in the first two cases, to give a numerical estimate of the fractal dimension.

The first, loop-erased random walks, belongs to the realm of “pure combinatorics”.

The second, percolation, is at the frontier between pure combinatorics and statistical mechanics because it arises very naturally as the domain boundary of a statistical mechanics model, but the Boltzmann weights are trivial. It is however a limiting case of a family of models with non trivial Boltzmann weights and, from that point of view, quantities relevant for percolation are obtained by exploring an infinitesimal neighborhood around the trivial Boltzmann weights.

The third example, the Ising model, is deeply rooted in statistical mechanics.

We shall end this section by abstracting a crucial property of interfaces which allows to make an efficient use of conformal invariance and derive the Markov property for SLEs.

1.1.1 Loop-erased random walks. This example is purely of combinatorial nature. A loop-erased random walk is a random walk with loops erased along as they appear. More formally, if X_0, X_1, \dots, X_n is a finite sequence of abstract objects, we define the associated loop-erased sequence by the following recursive algorithm.

Until all terms in the sequence are distinct,

Step 1 Find the couple (l, m) with $0 \leq l < m$ such that the terms with indexes from 0 to $m - 1$ are all distinct but the terms with indexes m and l coincide.

Step 2 Remove the terms with indexes from $l + 1$ to m , and shift the indexes larger than m by $l - m$ to get a new sequence.

Let us look at two examples.

For the “month” sequence $j, f, m, a, m, j, j, a, s, o, n, d$, the first loop is m, a, m , whose removal leads to $j, f, m, j, j, a, s, o, n, d$, then j, f, m, j , leading to j, j, a, s, o, n, d , then j, j leading to j, a, s, o, n, d where all terms are distinct.

For the “reverse month” sequence $d, n, o, s, a, j, j, m, a, m, f, j$, the first loop is j, j , leading to $d, n, o, s, a, j, m, a, m, f, j$, then a, j, m, a leading to d, n, o, s, a, m, f, j .

This shows that the procedure is not “time-reversal” invariant. Moreover, terms that are within a loop can survive: in the second example m, f , which stands in the j, m, a, m, f, j loop, survives because the first j is inside the loop a, j, m, a which is removed first.

A loop-erased random walk is when this procedure is applied to a (two dimensional for our main interest) random walk. This is very easy to simulate. Fig.1.2 represents a loop-erased walk of 200 steps. The thin lines build the shadow of the random walk (where shadow means that we do not keep track of the order and multiplicity of the visits) and the thick line is the corresponding loop-erased walk. The time asymmetry is clearly visible and allows to assert with little uncertainty that the walk starts on the left.

To fit with the general SLE framework, let us restrict to loop-erased random walks in the upper-half plane. There are a few options for the choice of boundary conditions.

A first choice is to consider reflecting boundary conditions on the real axis for the random walk.

Another choice is annihilating boundary conditions: if the random walk

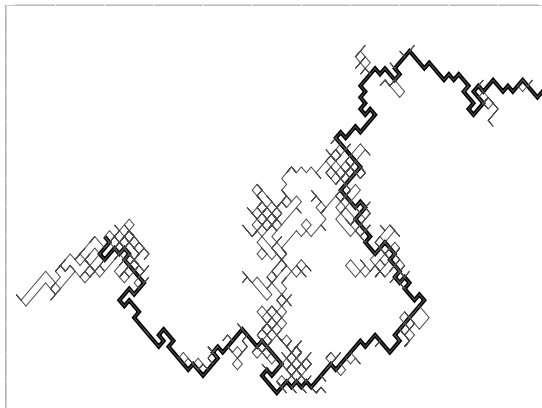


Figure 1.2 A loop-erased random walk with its shadow.

hits the real axis, one forgets everything and starts anew at the origin. Why this is a natural boundary condition has to wait until section 1.1.4.

Due to the fact that on a two-dimensional lattice a random walk is recurrent (with probability one it visits any site infinitely many times), massive rearrangement occur with probability one. This means that if one looks at the loop-erased random walk associated to a given random walk, it does not have a limit in any sense when the size of the random walk goes to infinity. Let us illustrate this point. The samples in fig.1.3 were obtained with reflecting boundary conditions. It takes 12697 random walk steps to build a loop-erased walk of length 633, but step 12698 of the random walk closes a long loop, and then the first occurrence of a loop-erased walk of length 634 is after 34066 random walk steps. Observe that in the mean time most of the initial steps of the loop-erased walk have been reorganized.

However, simulations are possible because when the length of the random walk tends to infinity, so does the maximal length of the corresponding loop-erased walk with probability one.

Though annihilating boundary conditions lead to remove even more parts of the random walk than the reflecting ones, the corresponding process can be arranged (conditioned in probabilistic jargon) to solve the problem of convergence as follows.

Instead of stopping the process when the loop-erased walk has reached a given length, one can stop it when it reaches a certain altitude, say n , along the y -axis. Whatever the corresponding random walk has been, the only thing that matters is the last part of it, connecting the ori-

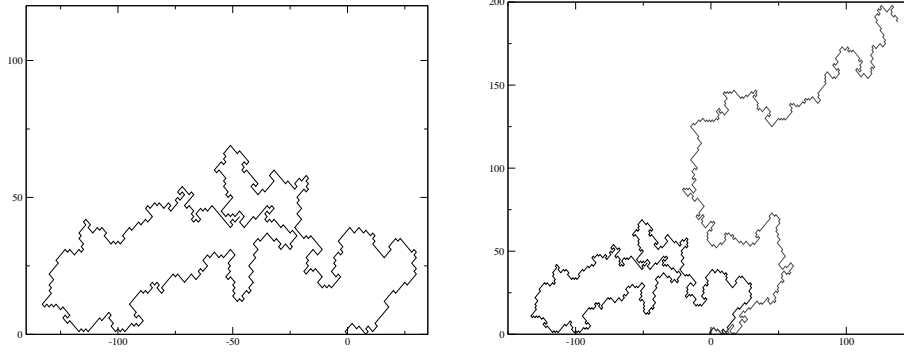


Figure 1.3 On the left: a large loop is about to be created. On the right: the massive rearrangement to go from 633 to 634 steps.

gin to altitude n without returning to altitude 0. Moreover, the first time the loop-erased walk reaches altitude n is exactly the first time the random walk reaches altitude n . Now a small miracle happens: if a 1d symmetric random walk is conditioned to reach altitude n before it hits the origin again, the resulting walk still has the Markov property. It is a discrete equivalent to the 3d Bessel process (a Bessel process describes the norm of a Brownian motion, however no knowledge of Bessel processes is needed here, we just borrow the name). When at site m , $0 < m < n$, the probability to go to $m \pm 1$ is $(1 \pm 1/m)/2$, independently of all previous steps. Observe that there is no n dependence so that we can forget about n , i.e. let it go to infinity. The discrete 3d Bessel process is not recurrent and tends to infinity with probability one: for any altitude l there is with probability one a time after which the discrete 3d Bessel process remains above l for ever. Henceforth, we choose to simulate a symmetric simple random walk along the x axis and the discrete 3d Bessel process along the y -axis and we erase the loops of this new process. This leads to the convergence of the loop-erased walk and numerically to a more economical simulation.

Fig.1.4 is a simulation of about 10^5 steps, both for reflecting and annihilating boundary conditions. At first glance, one observes in both cases similar simple (no multiple points) but irregular curves with possibly fractal behavior.

To estimate the Hausdorff dimensions in both cases, we have generated samples of random walks, erased the loops and made the statistics of the number of steps S of the resulting walks compared to a typical length L (end-to-end distance for reflecting boundary conditions, maximal altitude for annihilating boundary conditions). In both cases, one

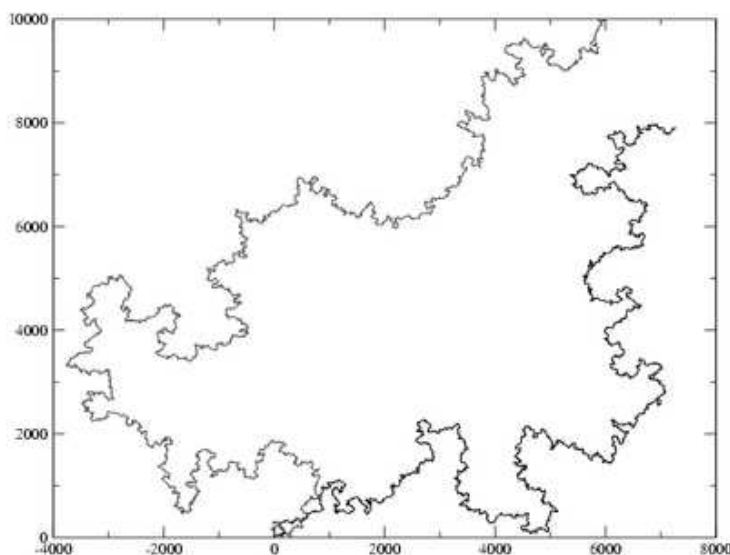


Figure 1.4 A sample of the loop-erased random walk for the two boundary conditions.

observes that $S \propto L^\delta$ and a modest numerical effort (a few hours of CPU) leads to $\delta = 1.25 \pm .01$. This is an indication that the boundary conditions do not change the universality class.

To get an idea of how small the finite size corrections are, observe fig.1.5. The altitude was sampled from 2^4 to 2^{13} . The best fit gives a slope 1.2496 and the first two points already give 1.2403.

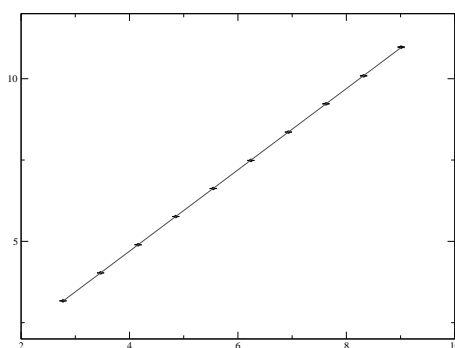


Figure 1.5 The logarithm of the average length of the loop-erased random walk versus logarithm of the maximum altitude. The numerical results are the circles, the straight line is the linear regression, the error bars are shown.

As recalled in the introduction, it is believed on the basis of intuitive arguments that in two dimensions scale invariance implies conformal invariance, providing there are no long range interactions. What does this absence of long range interactions mean for loop-erased random walks? Clearly along the loop-erased walk there are long range correlations, if only because a loop-erased random walk cannot cross itself. However, the relevant feature for the intuitive argument is that, in the underlying 2d physical space, interactions are indeed short range. At each time step, the increment of the underlying random walk is independent of the rest of the walk, and the formation of a loop to be removed is known from data at the present position of the random walk.

From the analytical viewpoint, the loop-erased random walk is one of the few systems that has been proved to have a conformally invariant distribution in the continuum limit, the fractal dimension being exactly $5/4$. A naive idea to get directly a continuum limit representation of loop-erased walks would be to remove the loops from a Brownian motion. This turns out to be impossible due to the proliferation of overlapping loops of small scale. However, the SLE_2 process, to be defined later, gives a direct definition. In fact, it is the consideration of loop-erased random walks that led Schramm [4] to propose SLE as a description of interfaces.

1.1.2 Percolation. To define a random interface for percolation, one possibility is to pave the upper-half plane with regular hexagons. Each one is, independently of the others, occupied or empty with probability $1/2$, with the exception of the ones along the real axis, which are all empty on the positive real axis and occupied on the negative real axis, see fig.1.6. Then a continuous interface, starting at the origin and separating occupied and unoccupied hexagons, is uniquely defined. As before, this defines a simple curve on the lattice.

The percolation interface has an obvious but very remarkable property that singles it out: *locality*. Locality means that the percolation interface does not depend on the distribution of occupied and empty sites away from itself. Equivalently, if \mathbf{D} is a domain (i.e. in this discrete setting a connected and simply connected family of hexagons in the upper half plane) containing the origin, the law of the percolation interface in \mathbf{D} before it hits the boundary of \mathbf{D} for the first time is independent of the distribution of occupied/empty sites outside \mathbf{D} . It is the same law as for what one would define as the percolation interface in \mathbf{D} without ever mentioning the world outside \mathbf{D} .

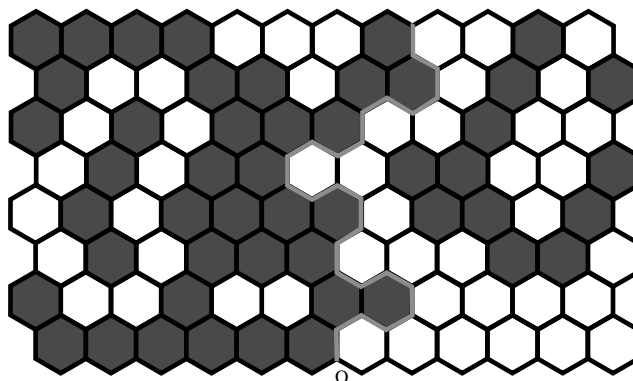


Figure 1.6 The definition of the percolation interface.

This observation makes the percolation interface easy to simulate. Indeed, the construction of a percolation interface proceeds inductively, as shown on the fig.1.7.

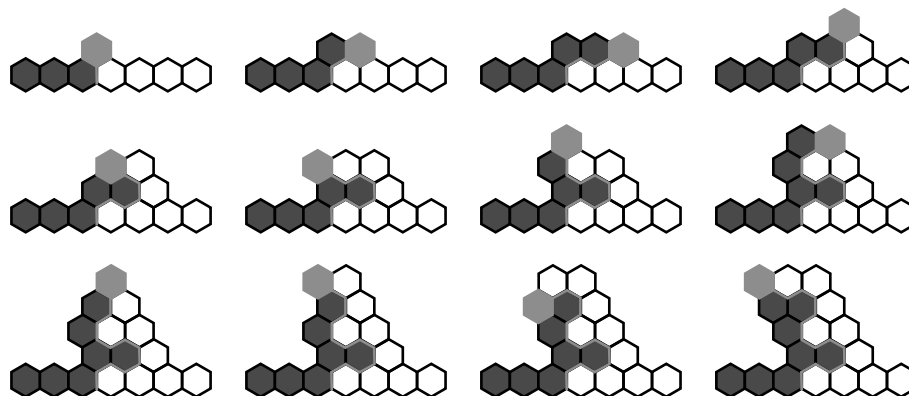


Figure 1.7 The percolation interface as a growth process.

Fig.1.8 shows a few samples of increasing size.

The contrast with the previous example is rather striking. Even for small samples, the percolation interface makes many twists and turns. With the resolution of the figure, the percolation interface for large samples does not look like a simple curve at all! The intuitive explanation why this does not occur for loop-erased walks is that if it comes close to

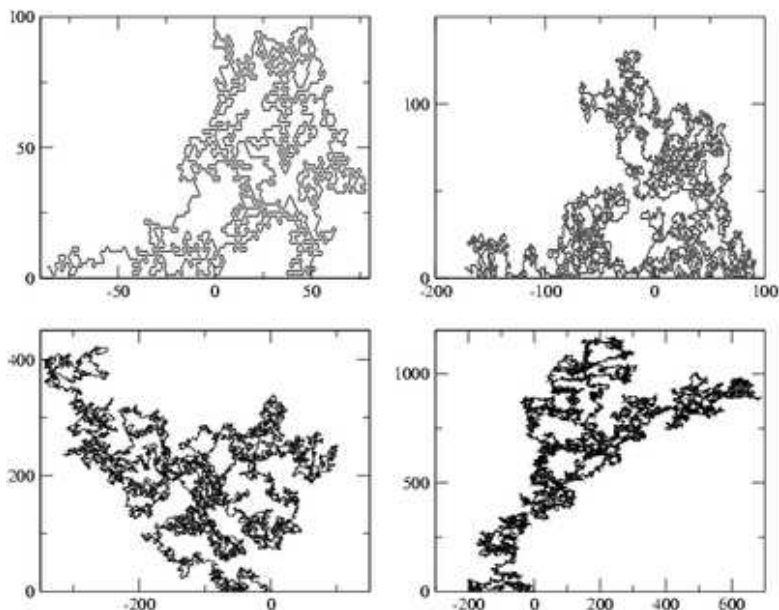


Figure 1.8 Samples of the percolation interface for increasing sizes.

itself, then with large probability a few more steps of the random walk will close a loop.

Getting an estimate of the fractal dimension of the percolation interface proceeds along lines similar to the first example. If the number of steps S of the percolation interface is compared to a typical length L one observes that $S \propto L^\delta$ and a modest numerical effort (a few hours of CPU) leads to $\delta = 1.75 \pm .01$.

The percolation interface is also built by applying rules involving only a few nearby sites, and again it is expected on general non rigorous arguments that its scale invariance should imply its conformal invariance in the continuum limit.

The percolation process is another one among the few systems that has been proved to have a conformally invariant distribution in the continuum limit, the fractal dimension being exactly $7/4$. As suggested by numerical simulations, the continuum limit does not describe simple curves but curves with a dense set of double points, and in fact the –to be defined later– SLE_6 process describes not only the percolation interface but also the percolation hull [2], which is the complement of the set of points that can be joined to infinity by a continuous path that does not intersect the percolation interface.

1.1.3 The Ising model. Our next example makes also use of the same pictorial representation: it is the Ising model on the triangular lattice in the low temperature expansion. The spins are fixed to be *up* on the left and down on the right of the origin along the real axis. The energy of a configuration is proportional to the length of the curves separating up and down islands. The proportionality constant has to be adjusted carefully to lead to a critical system with long range correlations. This time, making accurate simulations is much more demanding. On the square lattice, the definition of the interface suffers from ambiguities, but these become less relevant for larger sample sizes.

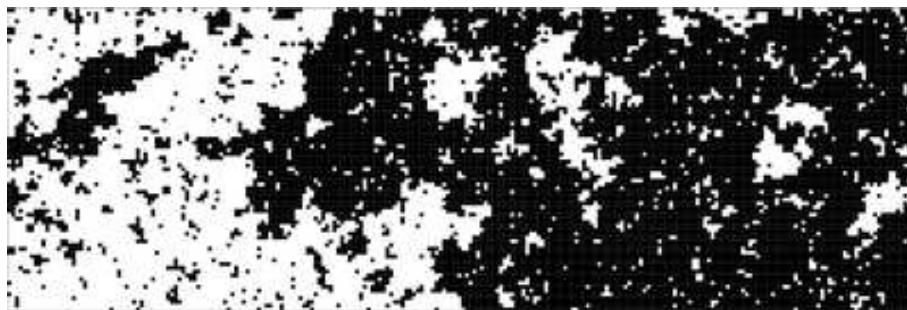


Figure 1.9 A sample for the critical Ising model. The bottom line, where the spins are frozen –black on the right, white on the left– is not represented. Courtesy of J. Houdayer.

Although there is no question that the fractal dimension of the Ising interface with the above boundary conditions is $11/8$ and is described by –to be defined later– SLE_3 , a mathematical proof that a continuum limit distribution for the interface exists and is conformally invariant is still out of reach.

We conclude this list of examples with two remarks.

First, the pictorial representation by a gas of non-intersecting curves on the hexagonal lattice that we used in the second and the third example applies to another family of models, the $O(n)$ models, to which similar interface considerations would apply.

Second, non branching interfaces, described on the lattice by simple curves, are not the generic situation. For instance the $Q = 3$ states Potts model, three different phases coexist and the physical interfaces have branch points.

1.1.4 A generality. Up to now, we have discussed interfaces in –lattice approximations of– the upper half plane. Let us note that they make sense for more general domains.

Start with the case of the percolation or of the Ising model. In the plane, take any connected and simply connected collection of hexagons, split it into an interior and a connected boundary, and split the boundary in two connected pieces in such a way that exactly two pairs of adjacent boundary hexagons, marked a and b , carry different colors, see fig.1.10. Observe that we allow a cut which would correspond to the beginning of the interface. Hexagons separated by the cut are not to be counted as neighbors.

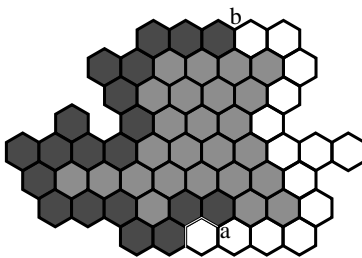


Figure 1.10 A domain on which percolation and the Ising model can be defined.

Then any coloring of the hexagons in the interior will lead to a well-defined interface. It will also lead to a well defined energy, and then the question of the distribution of the interface in such a domain is meaningful. For percolation the energy is independent of the configuration. For the Ising model, it is proportional to the length of the curves separating up and down sites. Observe that –as the possible cut separates fixed spins– counting interactions across the cut or not in the energy just adds a constant to it, so that it has no influence on probabilities.

For the loop-erased random case, the idea is similar. One takes a simply connected piece of the square lattice with two points a and b on the boundary, again allowing some cuts, see fig.1.11. Consider all walks from a to b that do not touch the boundary except at a before the first step and at b after the last step and give each such walk of length l a weight 4^{-l} . Observe that this choice is exactly the annihilating boundary condition: in the half plane geometry, a was the origin and b the point at infinity and, due to the infinite extension of the boundary, we had to go through a limiting procedure. Then erase the loops to get a probability distribution for loop-erased random walks from a to b in the domain. The probability for the simple symmetric random walk to hit the boundary

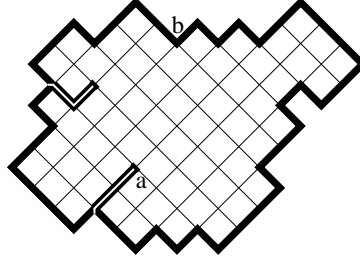


Figure 1.11 A domain on which loop-erased random walks can be defined.

for the first time at b starting from a can be interpreted as the partition function for loop-erased walks.

We can now go to the point we want to make, valid for all the above examples. For any of these, we use $P_{(\mathbf{D},a,b)}$ to denote the probability distribution for the interface $\gamma_{[ab]}$ from a to b in \mathbf{D} .

Suppose that we fix the beginning $\gamma_{[ac]}$ of a possible interface in domain \mathbf{D} , up to a certain point c . Then 1) we can consider the conditional distribution for the rest of the interface and 2) we can remove the beginning of the interface from the domain to create a new domain and consider the distribution of the interface in this new domain. This is illustrated on fig.1.12.

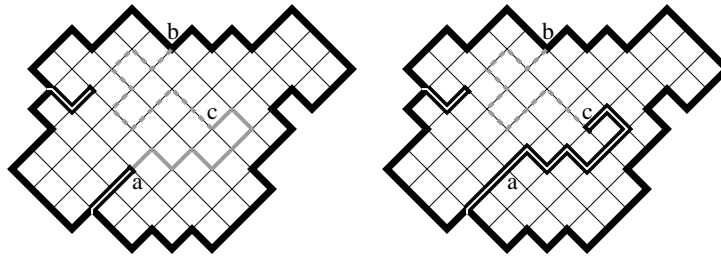


Figure 1.12 An illustration of situations 1) and 2) for the case of loop-erased walks. What is the distribution of the dotted curve in both situations ?

We claim that the distributions defined in 1) and 2) coincide. For reasons to be explained in a moment, we call this property “locality at the interface”. In equations

$$P_{(\mathbf{D},a,b)}(\cdot | \gamma_{[ac]}) = P_{(\mathbf{D} \setminus \gamma_{[ac]},c,b)}(\cdot).$$

It is obvious that these two probabilities are supported on the same set, namely simple curves along the edges of the lattice, going from c to b in $\mathbf{D} \setminus \gamma_{[ac]}$. Let us however note that for loop-erased random walks, annihilating boundary conditions are crucial. Reflecting boundary conditions clearly do not work, if only because the supports do not coincide in that case.

For the case of loop-erased random walks, the argument for the equivalence of 1) and 2) goes as follows. Take any random walk (possibly with loops) $W_0 = a, W_1, \dots, W_l = b$ that contributes to an interface $\gamma_{[ab]}$ which is $\gamma_{[ac]}$ followed by some $\gamma_{[cb]}$. Let m be the largest index for which the walk visits c . Because the interface has to start with $\gamma_{[ac]}$, the walk $W_m = c, \dots, W_l = b$ cannot cross $\gamma_{[ac]}$ again, so it is in fact a walk in $\mathbf{D} \setminus \gamma_{[ac]}$ from c to b leading to the interface $\gamma_{[cb]}$. The weight for the walk $W_0 = a, W_1, \dots, W_l = b$ is 4^{-l} , i.e. simply the product of weights for the walks $W_0 = a, W_1, \dots, W_m = c$ and $W_m = c, \dots, W_l = b$. Then a simple manipulation of weights leads directly to the announced result.

For the case of percolation and the Ising model, in fact more is true: we can view $P_{(\mathbf{D}, a, b)}$ not only as a probability distribution for the interface, but as the full probability distribution for the colors of the hexagons and still check the identity of 1) and 2). Again, the supports are the same for 1) and 2), namely any configuration of the colors, except that the colors on both sides of $\gamma_{[ac]}$ are fixed. For the case of percolation, the colors are independent of each other so the identity of 1) and 2) is clear. For the Ising model, the difference is that the conditional probabilities in 1) take into account the interactions between the colors along the interface, whereas the probability in 2) does not take into account the interactions between the spins along the cut left by the removal of the interface. However, as already mentioned above, the corresponding colors are fixed anyway, so the Boltzmann weights for the configurations that are in the support of 1) or 2) differ by a multiplicative constant, which disappears when probabilities are computed.

This argument extends immediately to systems with only nearest neighbor interactions. They can be defined on any graph. If any subset of edges is chosen and the configuration at both end of each edge is frozen, it makes no difference for probabilities to consider the model on a new graph in which the frozen edges have been deleted.

Instead of looking for further generalizations, we argue more heuristically that the continuum limit for a system with short range interactions should satisfy locality at the interface. The use of this locality property—which, as should be amply evident, has nothing to do with conformal

invariance— together with the conformal invariance assumption is at the heart of O. Schramm’s derivation of stochastic Loewner evolutions.

1.2 O. SCHRAMM’S ARGUMENT

We break the argument in several pieces. The heart of the probabilistic derivation establishes two properties of conformally invariant interfaces:

- the Markov property,
- the stationarity of increments,

see sections 1.2.3, 1.2.2 and 1.2.5. The crucial results needed for the probabilistic part, in particular the basics of Loewner evolutions, are collected in 1.2.1 and 1.2.4. The last two subsections are not directly related to the argument. They collect some basic facts on the fractal properties of SLE interfaces and on the connection with CFT.

1.2.1 Riemann’s theorem and hulls. In this section we collect a few indispensable results used in the rest of the course.

A domain is a non empty connected and simply connected open set strictly included in the complex plane \mathbf{C} . Simple connectedness is a notion of purely topological nature which in two dimensions asserts essentially that a domain has no holes and is contractible. But it is a deep theorem of Riemann that two domains are always conformally equivalent, i.e. there is an invertible holomorphic map between them. For instance, the upper-half plane \mathbf{H} is a domain. It is well known that it has a three dimensional Lie group of conformal automorphisms, $PSL_2(\mathbf{R})$, that also acts on the boundary of \mathbf{H} . There is a unique automorphism, possibly followed by a transposition, that maps any triple of boundary points to any other triple of boundary points. By Riemann’s theorem, this is also true for any other domain, at least if the boundary is not too wild.

Riemann’s theorem is used repeatedly in the rest of this course and is the starting point of many approaches to growth phenomena in two dimensions.

For later use, we note that one can be a bit more explicit when the domain \mathbf{D} differs only locally from the upper half plane \mathbf{H} , that is if $\mathbf{K} = \mathbf{H} \setminus \mathbf{D}$ is bounded. Such a set \mathbf{K} is called a hull. The real points in the closure of \mathbf{K} in \mathbf{C} form a compact set which we call $\mathbf{K}_{\mathbf{R}}$. Let $f : \mathbf{H} \mapsto \mathbf{D}$ be a conformal bijection. As the boundary of \mathbf{H} is smooth, f has a continuous extension to $\overline{\mathbf{R}} \equiv \mathbf{R} \cup \infty$, and $f^{-1}(\overline{\mathbf{R}} \setminus \mathbf{K}_{\mathbf{R}})$ is a non-empty open set in $\overline{\mathbf{R}}$ with compact complement. We call the complement the

cut of f . By the Schwarz symmetry principle, defining $f(z) = \overline{f(\bar{z})}$ for $\Im z \leq 0$ gives an analytic extension of f to the whole Riemann sphere minus the cut. Across the cut, f has a purely imaginary nonnegative discontinuity which we write as a Radon-Nikodym derivative $d\mu_f/dx$.

One can use the $PSL_2(\mathbf{R})$ automorphism group of \mathbf{H} to ensure that f is holomorphic at ∞ and $f(w) - w = O(1/w)$ there. This is called the hydrodynamic normalization. It involves three conditions, so there is no further freedom left. We shall denote this special representative by $f_{\mathbf{K}}$, which is uniquely determined by \mathbf{K} : any property of $f_{\mathbf{K}}$ is an intrinsic property of \mathbf{K} .

Cauchy's theorem yields

$$f_{\mathbf{K}}(w) = w + \frac{1}{2\pi} \int_{\mathbf{R}} \frac{d\mu_{f_{\mathbf{K}}}(x)}{x - w}, \quad (1.1)$$

A quantity that plays an important role in the sequel is

$$C_{\mathbf{K}} \equiv \frac{1}{2\pi} \int_{\mathbf{R}} d\mu_{f_{\mathbf{K}}}(x),$$

a positive (unless $\mathbf{K} = \emptyset$) number called the capacity of \mathbf{K} , which is such that $f_{\mathbf{K}}(w) = w - C_{\mathbf{K}}/w + O(1/w^2)$ at infinity. The usefulness of capacity stems from its good behavior under compositions: if \mathbf{K} and \mathbf{K}' are two hulls, $\mathbf{K} \cup f_{\mathbf{K}}(\mathbf{K}')$ is a hull and

$$C_{\mathbf{K} \cup f_{\mathbf{K}}(\mathbf{K}')} = C_{\mathbf{K}} + C_{\mathbf{K}'}, \quad (1.2)$$

as seen by straightforward expansion at infinity of $f_{\mathbf{K}} \circ f_{\mathbf{K}'}$, the map associated to $\mathbf{K} \cup f_{\mathbf{K}}(\mathbf{K}')$. In particular capacity is a continuous increasing function on hulls.

Anticipating a little bit, let us note immediately that giving a dynamical rule for the evolution of the finite positive measure $d\mu_{f_{\mathbf{K}}}(x)$ is a good way to define growth processes.

1.2.2 Conformally invariant interfaces. Consider a domain \mathbf{D} , with two distinct points on its boundary, which we call a and b . A simple curve, denoted by $\gamma_{[ab]}$, from a to b in \mathbf{D} is the image of a continuous one-to-one map γ from the interval $[0, +\infty]$ to $\mathbf{D} \cup \{a, b\}$ such that $\gamma(0) = a$, $\gamma(\infty) = b$ and $\gamma_{[ab]} \equiv \gamma([0, \infty]) \subset \mathbf{D}$. Alternatively, a simple curve from a to b is an equivalence class of such maps under increasing reparametrizations. A point on it has no preferred coordinate but it has a past and a future. If $c \in \mathbf{D}$ is an interior point, we use a similar definition for a simple curve $\gamma_{[ac]}$ from a to c in \mathbf{D} .

Note that, apart from the fact that on the lattice we could use lattice length as a parameter along the interface, we have just rephrased in the continuum –but with the same notations– what we did before in a discrete setting.

Our aim is to study conformally invariant probability measures on the set of simple curves from a to b in \mathbf{D} . There is a purely kinematical step, which demands that if h is any conformal map that sends \mathbf{D} to another domain $h(\mathbf{D})$, the measure for $(h(\mathbf{D}), h(a), h(b))$ should be the image by h of the measure for (\mathbf{D}, a, b) :

$$P_{(\mathbf{D}, a, b)}(\gamma_{[ab]} \subset U) = P_{(h(\mathbf{D}), h(a), h(b))}(h(\gamma_{[ab]}) \subset h(U)),$$

where $P_{(\mathbf{D}, a, b)}(\gamma_{[ab]} \subset U)$ denotes the probability for the curve $\gamma_{[ab]}$ to remain in a subset U of \mathbf{D} . See fig.1.13.

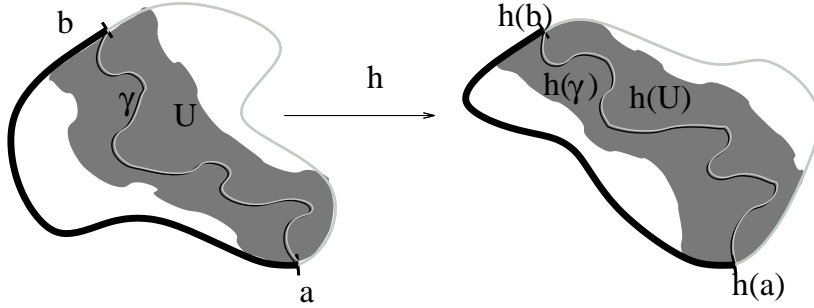


Figure 1.13 Conformal invariance for change of domain.

This condition is natural and it is the one that conformal field theory suggests immediately. Let us note however that a totally different definition of conformal invariance is understood in the familiar statement “two dimensional Brownian motion is conformally invariant”.

Observe that we could take any measure for (\mathbf{D}, a, b) –well, with the invariance under the one parameter group of automorphisms that fixes (\mathbf{D}, a, b) – and declare that the measure in $h(\mathbf{D})$ is obtained by definition by the rule above. To make progress, we need to combine conformal invariance with locality at the interface.

1.2.3 Markov property and stationarity of increments. This short section establishes the most crucial properties of conformally invariant interfaces.

Take $c \in \mathbf{D}$ and let $\gamma_{[ac]}$ be a simple curve from a to c in \mathbf{D} . Observe that $\mathbf{D} \setminus \gamma_{[ac]}$ is a domain. To answer the question “if the beginning of the interface is fixed to be $\gamma_{[ac]}$, what is the distribution of the rest $\gamma'_{[cb]}$ ”

of the interface ?” we apply locality at the interface to argue that this is exactly the distribution of the interface in $\mathbf{D} \setminus \gamma_{[ac]}$. We map this domain conformally to \mathbf{D} via a map h_γ sending b to b and c to a , see fig.1.14.

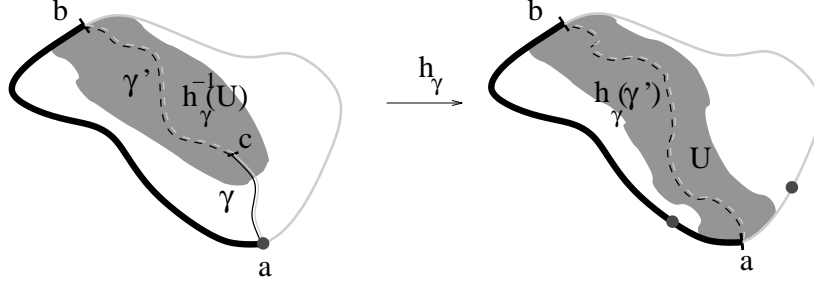


Figure 1.14 Conformal invariance for conditional probabilities.

Conformal invariance implies that the image measure is the original measure in $P_{(\mathbf{D}, a, b)}$, where $h_\gamma(\gamma'_{[cb]})$ is an interface that has forgotten $\gamma_{[ac]}$. To summarize :

$h_\gamma(\gamma'_{[cb]})$ is independent of $\gamma_{[ac]}$ (the Markov property) and has the same distribution as the original interface itself (stationarity of increments).

1.2.4 Local growth and Loewner evolutions. The Markov and stationarity of increments property make it plain that to understand the distribution of the full interface, it is enough to understand the distribution of a small, or even infinitesimal, initial segment, and then glue segments via conformal maps.

This calls for a description by differential equations.

For this purpose, it is very convenient –even if by no means mandatory– to have a natural parametrization of interfaces. Using conformal invariance, we can restrict ourselves to the situation when $(\mathbf{D}, a, b) = (\mathbf{H}, 0, \infty)$. If $\gamma_{[0, \infty]}$ is a simple curve from 0 to ∞ in \mathbf{H} , and c a point on it, we know that $\mathbf{H} \setminus \gamma_{[0, c]}$ is a domain, and $\gamma_{[0, c]}$ itself is a hull. We use capacity as a parametrization and define a time parameter by $2t(c) \equiv C_{\gamma_{[0, c]}}$. The factor of 2 is just historical. The map t is a continuous increasing function of c varying from 0 to ∞ in \mathbf{R} when c moves from 0 to ∞ along $\gamma_{[0, \infty]}$. The inverse map $t \mapsto c(t)$ is well-defined and gives a parametrization of the curve. So we introduce an increasing family of hulls $\mathbf{K}_t, t \in [0, \infty[$, by $\mathbf{K}_t = \gamma_{[0, c(t)]}$ which has capacity $2t$. Let $f_t \equiv f_{\mathbf{K}_t}$ be the conformal homeomorphism from \mathbf{H} to $\mathbf{H} \setminus \mathbf{K}_t$ normalized to sat-

isfy $f_t(w) = w - 2t/w + O(1/w^2)$ at infinity. Define $g_t : \mathbf{H} \setminus \mathbf{K}_t \mapsto \mathbf{H}$ to be the inverse of f_t . Then $g_t(z) = z + 2t/z + O(1/z^2)$ at infinity.

To study the evolution of the family of hulls \mathbf{K}_t , fix $\varepsilon \geq 0$ and consider the hull $\mathbf{K}_{\varepsilon,t} \equiv g_t(\mathbf{K}_{t+\varepsilon} \setminus \mathbf{K}_t)$, which has capacity 2ε by eq.(1.2). Define $f_{\varepsilon,t} \equiv f_{\mathbf{K}_{\varepsilon,t}}$. Then $g_t = f_{\varepsilon,t} \circ g_{t+\varepsilon}$ on $\mathbf{H} \setminus \mathbf{K}_{t+\varepsilon}$. Using the representation of $f_{\mathbf{K}_{\varepsilon,t}}$ in terms of its discontinuity eq.(1.1), we obtain

$$g_{t+\varepsilon} - f_{\varepsilon,t} \circ g_{t+\varepsilon} = g_{t+\varepsilon} - g_t = \frac{1}{2\pi} \int_{\mathbf{R}} \frac{d\mu_{f_{\varepsilon,t}}(x)}{g_{t+\varepsilon} - x}$$

We introduce now the notion of local growth which is crucial for interfaces. When ε is small, $\mathbf{K}_{\varepsilon,t}$ is a tiny piece of curve and the support of $d\mu_{f_{\varepsilon,t}}$ is small and becomes a point when ε goes to 0. Measures supported at a point are δ functions, so there is a point ξ_t such that, as a measure, $d\mu_{f_{\varepsilon,t}}/dx \sim 2\varepsilon\delta(x - \xi_t)$ as $\varepsilon \rightarrow 0^+$. If \mathbf{K}_t is a more general increasing family of hulls of capacity $2t$, we say that the condition of local growth is satisfied if the above small ε behavior holds. At first sight, it might seem that local growth is only true for curves, but this is not true. We shall give an example below.

Letting $\varepsilon \rightarrow 0^+$, from the local growth condition, we infer the existence of a real function ξ_t such that

$$\frac{dg_t}{dt}(z) = \frac{2}{g_t(z) - \xi_t}. \quad (1.3)$$

It is useful to look at this equation from a slightly different point of view, taking the function ξ_t as the primary data. The solutions of this equation for a given function ξ_t with initial condition $g_0(z) = z$ is called a Loewner evolution. The image of ξ_t by g_t^{-1} is the tip of the curve at time t .

The cases when the local growth condition is not satisfied are called Loewner chains, see below. Had we used another parametrization of the curve, the 2 in the numerator would be replaced by a positive function of the parameter along the curve.

Informally, if \mathbf{K}_t is a growing curve, we expect that $g_{t+\varepsilon}(z) - g_t(z)$ describes an infinitesimal cut. This is confirmed by the explicit solution of eq.(1.3) for the trivial case $\xi_t \equiv 0$, which yields $g_t(z)^2 = z^2 + 4t$, the branch to be chosen being such that at large z , $g_t(z) \sim z$. This describes a growing segment along the imaginary axis. So intuitively, the simple pole in eq.(1.3) accounts for the existence of a cut and different functions ξ_t account for the different shapes of curves.

One can also solve the case when \mathbf{K}_t is an arc of circle starting from the origin. It can be obtained from the trivial solution above by applying appropriate time dependent $PSL_2(\mathbf{R})$ transformations both to g_t and z

and then by a time change to recover the capacity parametrization. This is an illuminating exercise that we leave to the reader. Take an arc going from 0 to $2R$ along a circle of radius R . It turns out that when the arc approaches the real axis to close a half disk, the function ξ_t has a square root singularity $\xi_t \propto \sqrt{R^2 - 2t}$. The capacity remains finite and goes to R^2 and the map itself has a limit $g_{R^2/2}(z) = z + R^2/(z + R)$ which has swallowed the half disk without violating the local growth condition. One can start the growth process again. Making strings of such maps with various values of the radii is a simple way to construct growing families of hulls that are not curves and that nevertheless grow locally. Note that a square root singularity for ξ_t is the marginal behavior: if ξ_t is Hölder of exponent $> 1/2$, Loewner evolution yields a simple curve.

1.2.5 Stochastic (or Schramm) Loewner evolutions. If we sample locally growing hulls with a certain distribution, we get an associated random process ξ_t . In the case of a conformally invariant distribution, we have established two crucial properties: Markov property and stationarity of increments. To finish Schramm's argument leading to SLE, what remains is to see the implications of these properties on the distribution of ξ_t .

The argument and expressions for the meaning of Markov property and stationarity of increments involved a map h that mapped the tip of the piece of interface to the initial marked point a and the final marked point b to itself. The map $h_t(z) = g_t(z) - \xi_t$ has the required property when the domain is the upper-half plane with 0 and ∞ as marked points. It behaves like $h_t(z) = z - \xi_t + 2t/z + O(1/z^2)$ at infinity. We infer that for $s > t$, $h_t(\mathbf{K}_s \setminus \mathbf{K}_t)$ is independent of $\mathbf{K}_{t'}$, $t' \leq t$ (Markov property) and is distributed like a hull of capacity $s - t = C_{h_t(\mathbf{K}_s \setminus \mathbf{K}_t)}$ (stationarity of increments).

The hull determines the corresponding map h , so this can be rephrased as: $h_s \circ h_t^{-1}$ (which uniformizes $h_t(\mathbf{K}_s \setminus \mathbf{K}_t)$) is independent of $h_{t'}$, $t' \leq t$, and distributed like an h_{s-t} . As $h_s \circ h_t^{-1} = z - (\xi_s - \xi_t) + (s-t)/z + O(1/z^2)$ at infinity, the driving parameter for the process $h_s \circ h_t^{-1}$ is $\xi_s - \xi_t$. To summarize:

the Markov property and stationarity of increments for the interface lead to the familiar statement for the process ξ_t : for $s > t$, $\xi_s - \xi_t$ is independent of $\xi_{t'}$, $t' \leq t$, (Markov property) and distributed like a ξ_{s-t} (stationarity of increments).

To conclude, a last physical input is needed: one demands that the interface does not branch, which means that at two nearby times the

growth is at nearby points. This implies that ξ_t is a continuous process, in the sense that it has continuous trajectories.

One is now in position to apply a mathematical theorem: a 1d Markov process with continuous trajectories and stationary increments is proportional to a Brownian motion. We conclude that there is a real positive number κ such that $\xi_t = \sqrt{\kappa}B_t$ for some normalized Brownian motion B_t with covariance $\mathbf{E}[B_s B_t] = \min(s, t)$. The same argument without imposing that the time parametrization is given by the capacity of the hull would lead to the conclusion that the driving parameter is a continuous martingale, which is nothing but a Brownian motion after a possibly random time change.

A solution of

$$\frac{dg_t}{dt}(z) = \frac{2}{g_t(z) - \sqrt{\kappa}B_t} \quad (1.4)$$

is called a chordal Schramm-Loewner evolution of parameter κ , in short a chordal SLE $_{\kappa}$. The connection of this equation with interfaces relies mainly on conformal invariance. But local growth, absence of branches and to a lower level locality at the interface also play a crucial role.

1.2.6 Miscellanea on SLE. Up to now we have only discussed the situation when the interface goes from 0 to ∞ in the upper half plane, or more generally from one point on the boundary of a domain to another one. This is called chordal SLE. The argument can be extended easily to two other situations. The first is for an interface starting at a fixed point on the boundary of a domain and ending at a fixed point in the bulk. This is called radial SLE. For the second situation, three points are chosen on the boundary and the interface starts from the first point and ends at a random point between the two others. This is called dipolar SLE. Just as the upper-half plane is a convenient geometry for chordal SLE, a semi infinite cylinder is nice for radial SLE and an infinite strip is nice for dipolar SLE.

For radial SLE on a cylinder of circumference π , the equation reads

$$\frac{dg_t}{dt}(z) = \frac{2}{\tan(g_t(z) - \sqrt{\kappa}B_t)} \quad (1.5)$$

and for dipolar SLE on a strip of width $\pi/2$, one has

$$\frac{dg_t}{dt}(z) = \frac{2}{\tanh(g_t(z) - \sqrt{\kappa}B_t)} \quad (1.6)$$

The generalization of SLE to Riemann surfaces with moduli is easy for the annulus, but raises non-trivial problems in general, currently subject of active research.

The set of exact results obtained for SLE forms an impressive body of knowledge. We shall not mention the ones dealing with the explicit computation of certain crossing probabilities but we list just a few “pictorial” properties with some comments. They (the properties and the comments) should be understood with the standard proviso “almost surely” or “with probability 1”.

We start with a surprisingly difficult result [4, 5, 6, 7].

- Whatever the value of κ , the pre-image of the driving parameter $\lim_{w \rightarrow \sqrt{\kappa}B_t} g_t^{-1}(w)$ is a continuous curve γ_t , called the SLE trace. The trace never crosses itself. This property is crucial if the trace is to be interpreted as a curve separating two phases.
- For $\kappa \in [0, 4]$ the SLE trace is a simple curve. For $\kappa \in]4, 8[$, it has double points. For $\kappa \in [8, \infty[$, it is space filling.
- The fractal dimension d_κ of the trace is $1 + \kappa/8$ for $\kappa \leq 8$ and 2 for $\kappa \geq 8$.

Using the formula for the dimension of the trace and confronting with the numerical simulations, it is plausible (actually, these are among the few cases for which a mathematical proof exists) that loop-erased random walks correspond to $\kappa = 2, d = 5/4$ and percolation to $\kappa = 6, d = 7/4$. This is also compatible with the general shape of the numerical samples, which indicate that loop-erased random walks indeed lead to simple curves and that percolation doesn't.

The hull \mathbf{K}_t is by definition $\mathbf{H} \setminus g_t^{-1}(\mathbf{H})$. It has the following properties

- The hull \mathbf{K}_t is the complement of the connected component of ∞ in $\mathbf{H} \setminus \gamma_{[0,t]}$.
- For $\kappa \in [0, 4]$, the SLE hull is a simple curve coinciding with the trace. For $\kappa \in]4, \infty[$, the SLE hull has a nonempty connected and relatively dense interior.

This may seem surprising at first sight. It is the sign that for $\kappa > 4$, the drift $\sqrt{\kappa}B_t$ goes fast enough for the swallowing procedure to take place, as described in the closing arc example, but on all scales.

This is summarized by fig.1.15.

For the many other properties known about SLE, the reader is invited to read the vast literature [4, 5, 6, 7, 8, 9].

1.3 SHORT REMARKS ON SLE AND CFT

As already mentioned, it is by no means an easy task to prove that a discrete random curve converges to an SLE. For geometric models like

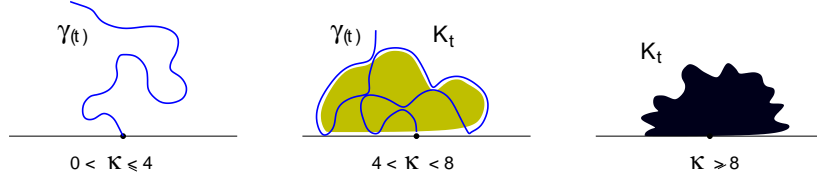


Figure 1.15 The phases of SLE.

percolation, loop-erased random walks, self avoiding walks, it is often easier to compute the appropriate κ using known special properties of the discrete model that are expected to survive in the continuum limit.

For instance, one can formulate locality in the continuum. Showing that SLE_κ has the locality property only for $\kappa = 6$ is a standard computation in stochastic Ito calculus, see e.g. [9].

For critical statistical mechanics models with non trivial Boltzmann weights, things are more complicated. The system contains local dynamical degrees of freedom independently from the interface and, in the continuum limit, these local degrees of freedom are expected to be described by a conformal field theory (CFT). The most basic parameter of a CFT is its central charge c . Computing it (even non rigorously) from the lattice model can be a challenge comparable to the one of computing κ .

On the other hand, the relation between c and κ can be worked out in general. The idea is elementary. From a technical viewpoint, it rests on assumptions similar to the ones needed in O. Schramm's argument.

In the discrete setting, take O to be any observable. If one computes $\langle O \rangle_{\mathbf{D} \setminus \gamma_{[ac]}}$ in $\mathbf{D} \setminus \gamma_{[ac]}$, i.e. with part of the interface fixed, and then averages over $\gamma_{[ac]}$ one retrieves $\langle O \rangle_{\mathbf{D}}$:

$$\mathbf{E}[\langle O \rangle_{\mathbf{D} \setminus \gamma_{[ac]}}] = \langle O \rangle_{\mathbf{D}}$$

where the expectation is the average over γ , see the last reference in [10]. This is a straightforward application of the usual rules of statistical mechanics

This basic property, which we call the martingale property because in probabilistic jargon it would be translated as “ $\langle O \rangle_{\mathbf{D} \setminus \gamma_{[ac]}}$ is a closed martingale for any observable O ” is expected to survive in the continuum limit. In this limit, one has two powerful tools inherited from conformal invariance at hand, CFT to compute correlators and SLE to average over the piece of interface. Doing this for arbitrary values of κ and c means mixing the degrees of freedom from two different models and there is a priori no reason for the martingale property to hold. An explicit

computation shows that it holds only if

$$2\kappa c = (6 - \kappa)(3\kappa - 8).$$

The martingale property also gives information on the operator content of the CFT. As the discrete statistical mechanics examples show, there is a change in boundary conditions at the tip of the interface. The martingale property allows to identify this boundary changing condition operator as a primary field of weight $h = (6 - \kappa)/(2\kappa)$ degenerate at level two.

This approach also exhibits a family of martingales which are at the heart of many probabilistic computations. For instance, it gives a systematic way to interpret probabilities for SLE events as correlation functions of a CFT, and shows how the changes of behavior of the trace at $\kappa = 4, 8$ are related to operator product expansions. The interested reader is referred to [10].

2. LOEWNER CHAINS

This section deals with more general 2D growth processes. Although, they do not fulfill the local growth and conformal invariance properties of SLEs, they are nevertheless described by dynamical conformal maps. We first present systems whose conformal maps have a time continuous evolution and give examples. We then go on by presenting a discrete version thereof in terms of iterated conformal maps. We explain integrability of Laplacian growth. The last part is a discussion concerning the limit of small ultraviolet cutoff and the consequences of possible dendritic anomalies.

2.1 CONTINUOUS LOEWNER CHAINS

In this part, the exterior of the unit disk is used as the reference geometry.

2.1.1 Radial Loewner chains. Let \mathbf{K}_t be a family of growing closed planar domains with the topology of a disk. Let $\mathbf{O}_t \equiv \mathbf{C} \setminus \mathbf{K}_t$ be their complements in the complex plane. See Figure (1.16). To fix part of translation invariance we assume that the origin belongs to \mathbf{K}_t and the point at infinity to \mathbf{O}_t .

Loewner chains describe the evolution of family of conformal maps f_t uniformizing $\mathbf{D} = \{w \in \mathbf{C}; |w| > 1\}$ onto \mathbf{O}_t . It thus describes the evolution of the physical domains \mathbf{O}_t . We normalize the maps $f_t : \mathbf{D} \rightarrow \mathbf{O}_t$ by demanding that they fix the point at infinity, $f_t(\infty) = \infty$ and

that $f'_t(\infty) > 0$. With t parameterizing time, Loewner equation reads:

$$\frac{\partial}{\partial t} f_t(w) = w f'_t(w) \oint \frac{du}{2i\pi u} \left(\frac{w+u}{w-u} \right) \rho_t(u) \quad (1.7)$$

The integration is over the unit circle $\{u \in \mathbf{C}, |u| = 1\}$. The Loewner density $\rho_t(u)$ codes for the time evolution. It may depends on the map f_t in which case the growth process is non-linear. For the inverse maps $g_t \equiv f_t^{-1} : \mathbf{O}_t \rightarrow \mathbf{D}$, Loewner equation reads:

$$\frac{\partial}{\partial t} g_t(z) = -g_t(z) \oint \frac{du}{2i\pi u} \left(\frac{g_t(z)+u}{g_t(z)-u} \right) \rho_t(u) \quad (1.8)$$

The behavior of f_t at infinity fixes a scale since at infinity, $f_t(w) \simeq R_t w + O(1)$ where $R_t > 0$, with the dimension of a `[length]`, is called the conformal radius of \mathbf{K}_t viewed from infinity. R_t may be used to analyze scaling behaviors, since Koebe 1/4-theorem (see e.g. [13]) ensures that R_t scales as the size of the domain. In particular, the (fractal) dimension D of the domains \mathbf{K}_t may be estimated by comparing their area \mathcal{A}_t with their linear size measured by R_t : $\mathcal{A}_t \asymp R_t^D$ for large t – the proportionality factor contains a cutoff dependence which restores naive dimensional analysis.

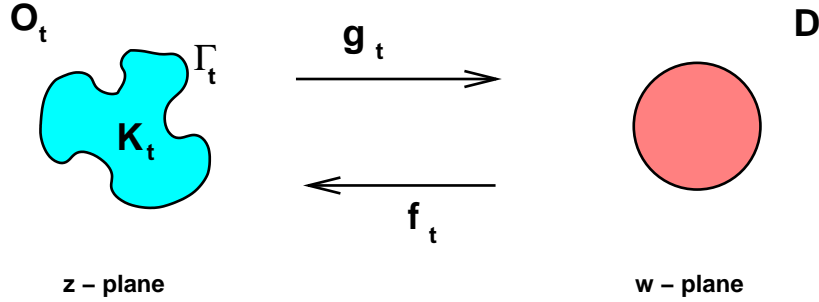


Figure 1.16 Uniformizing maps intertwining the ‘physical’ z -plane and the ‘mathematical’ w -plane.

2.1.2 The boundary curves. The boundary curve $\Gamma_t \equiv \partial \mathbf{O}_t$ is the image of the unit circle by f_t . We may parameterize the boundary points by $\gamma_{t;\alpha} = f_t(u)$ with $u = e^{i\alpha}$. The Loewner equation codes for the evolution of the shape of \mathbf{O}_t and thus for the normal velocity of the boundary points. Only the normal velocity is relevant as the tangent velocity is parameterization dependent. The tangent to the curve is

$\tau = iuf'_t(u)/|f'_t(u)|$ and the outward normal is $n = -i\tau$ so that the normal velocity at γ_t is $v_n = \Re[\bar{n} \partial_t f_t(u)]$, or

$$v_n = |f'_t(u)| \Re[\partial_t f_t(u)/uf'_t(u)].$$

The r.h.s. is determined by the Loewner equation (1.7) because this equation may be viewed as providing the solution of a boundary value problem. Indeed, recall that for $\hat{h}(u)$ a real function on the unit circle, $h(w) = \oint \frac{du}{2i\pi u} \left(\frac{w+u}{w-u} \right) \hat{h}(u)$ is the unique function analytic outside the unit disk whose real part on the unit circle is \hat{h} , i.e. $\Re[h(u)] = \hat{h}(u)$. Thus, since $\partial_t f_t(w)/wf'_t(w)$ is analytic in \mathbf{D} , the Loewner equation (1.7) is equivalent to:

$$v_n = |f'_t(u)| \rho_t(u)$$

or more explicitly ¹:

$$(\partial_\alpha \gamma_{t;\alpha}) (\partial_t \overline{\gamma_{t;\alpha}}) - (\partial_\alpha \overline{\gamma_{t;\alpha}}) (\partial_t \gamma_{t;\alpha}) = 2i |f'_t(u)|^2 \rho_t(u) \quad (1.9)$$

Hence, the evolution of the domain may be encoded either in the evolution law for its uniformizing conformal map as in eq.(1.7) or in the boundary normal velocity as in eq.(1.9). The two equations are equivalent.

2.2 EXAMPLES

2.2.1 Stochastic Loewner evolution (SLE). From this point of view, SLE is singular as it corresponds to a Dirac measure $\delta_{U_t}(u)$ centered at the position of a Brownian motion on the unit circle. The locality of this measure reflects the fact that SLE describes growing curves. Continuity of the Brownian motion reflects the absence of branching in the SLE growths. To make contact with the previous sections, the reader should check that eq.(1.5) becomes of the form (1.8) after the cylinder has been mapped to the outside of the unit disk.

2.2.2 Laplacian growth (LG). This is a process in which the growth of the domain is governed by the solution of Laplace equation, i.e. by an harmonic function, in the exterior of the domain with appropriate boundary conditions. It originates from the hydrodynamical Hele-Shaw problem to be described below.

To be precise, let P be the real solution of Laplace equation, $\nabla^2 P = 0$, in \mathbf{O}_t with the boundary behavior $P = -\log |z| + \dots$ at infinity and $P =$

¹For SLE this equation has to be modified according to Itô calculus

0 on the boundary curve $\Gamma_t = \partial\mathbf{O}_t$. The time evolution of the domain is then defined by demanding that the normal velocity of points on the boundary curve be equal to minus the gradient of P : $v_n = -(\nabla P)_n$.

This problem may be written as a Loewner chain since, as is well known, Laplace equation is solved via complex analysis by writing P as the real part of an analytic function. One first solves Laplace equation in the complement of the unit disk with the appropriate boundary conditions and then transports it back to the physical domain \mathbf{O}_t using the map f_t . This gives:

$$P = -\Re \Phi_t \quad \text{with} \quad \Phi_t(z) = \log g_t(z)$$

The evolution equation for the map f_t is derived using that the boundary normal velocity is $v_n = -(\nabla P)_n$. The above expression for P gives:

$$v_n = -(\nabla P)_n = |f'_t(u)|^{-1}$$

at point $\gamma_t = f_t(u)$ on the boundary curve. As explained in the previous section, this is enough to determine $\partial_t f_t(w)$ for any $|w| > 1$ since this data specifies the real part on the unit circle of the analytic function $\partial_t f_t(w)/w f'_t(w)$ on the complement of the unit disk. The result is:

$$\partial_t f_t(w) = w f'_t(w) \oint_{|u|=1} \frac{du}{2i\pi u |f'_t(u)|^2} \left(\frac{w+u}{w-u} \right) \quad (1.10)$$

It is a Loewner chain with $\rho_t(u) = |f'_t(u)|^{-2}$.

As we shall see below, Laplacian growth is an integrable system, which may be solved exactly, but it is ill-posed as the domain develops singularities (cusps $y^2 \simeq x^3$) in finite time. It thus needs to be regularized. There exist different ways of regularizing it.

One may also formulate Laplacian growth using a language borrowed from electrostatics by imagining that the inner domain is a perfect conductor. Then $V = \Re \Phi_t$ is the electric potential which vanishes on the conductor but with a charge at infinity. The electric field $\vec{E} = \vec{\nabla} V$ is $\vec{E} \equiv E_x - iE_y = \partial_z \Phi_t$. Its normal component $E_n = |f'_t(u)|^{-1}$ is proportional to the surface charge density.

2.2.3 The Hele-Shaw problem (HS). This provides a hydrodynamic regularization of Laplacian growth. The differences with Laplacian growth are in the boundary conditions which now involve a term proportional to the surface tension. It may be formulated as follows [14].

One imagines that the domain \mathbf{K}_t is filled with a non viscous fluid, say air, and the domain \mathbf{O}_t with a viscous one, say oil. Air is supposed to be injected at the origin and there is an oil drain at infinity. The pressure in

the air domain \mathbf{K}_t is constant and set to zero by convention. In \mathbf{O}_t the pressure satisfies the Laplace equation $\nabla^2 P = 0$ with boundary behavior $P = -\phi_\infty \log |z| + \dots$ at infinity reflecting the presence of the oil drain. The boundary conditions on the boundary curve are now $P = -\sigma \kappa_t$ with σ the surface tension and κ_t the curvature of the boundary curve². The fluid velocity in the oil domain \mathbf{O}_t is $\vec{v} = -\vec{\nabla} P$. Laplace equation for P is just a consequence of incompressibility. The evolution of the shape of the domain is specified by imposing that this relation holds on the boundary so that the boundary normal velocity is $v_n = -(\nabla P)_n$ as in Laplacian growth.

Compared to Laplacian growth, the only modification is the boundary condition on the boundary curve. This term prevents the formation of cusps with infinite curvature singularities. The parameter ϕ_∞ sets the scale of the velocity at infinity. In the following we set $\phi_\infty = 1$. By dimensional analysis this implies that `[time]` scales as `[length]2` and the surface tension σ has dimension of a `[length]`. It plays the role of an ultraviolet cut-off.

A standard procedure [14] to solve the equations for the Hele-Shaw problem is by first determining the pressure using complex analysis and then computing the boundary normal velocity. By Laplace equation, the pressure is the real part of an analytic function, $P = -\Re \Phi_t$. The complex velocity $v = v_x + iv_y$ is $\bar{v} = \partial_z \Phi_t$. At infinity $\Phi_t(z) \simeq \log z + \dots$ and $\bar{v} \simeq 1/z + \dots$. The boundary conditions on P demand that

$$(\Phi_t \circ f_t)(w) = \log w + \sigma \vartheta_t(w)$$

where $\vartheta_t(w)$ is analytic in \mathbf{D} with boundary value $\Re[\vartheta_t(u)] = \kappa_t(f_t(u))$ with κ_t the curvature. Explicitly

$$\vartheta_t(w) = \oint \frac{du}{2i\pi u} \left(\frac{w+u}{w-u} \right) \kappa_t(f_t(u))$$

The evolution of f_t is then found by evaluating the boundary normal velocity $v_n = \Re(\nabla \Phi)_n$ at point $\gamma_t = f_t(u)$:

$$v_n = \Re[n \partial_z \Phi_t] = |f'_t(u)|^{-1} \Re[1 + \sigma u \partial_u \vartheta_t(u)]$$

As above, this determines uniquely $\partial_t f_t(u)$ and it leads to a Loewner chain (1.7) with density:

$$\rho_t(u) = |f'_t(u)|^{-2} \left(1 + \sigma \epsilon_t(u) \right) \quad , \quad \epsilon_t(u) = \Re[u \partial_u \vartheta_t(u)] \quad (1.11)$$

²The curvature is defined by $\kappa \equiv -\vec{n} \cdot \partial_s \vec{\tau} / \vec{\tau}^2 = \Im[\bar{\tau} \partial_s \tau / |\tau|^3]$ with $\vec{\tau}$ the tangent and \vec{n} the normal vectors. An alternative formula is: $\kappa = |f'_t(u)|^{-1} \Re[1 + \frac{u f''_t(u)}{f'_t(u)}]$. For a disk of radius R , the curvature is $+1/R$.

The difference with Laplacian growth is in the extra term proportional to σ . It is highly non-linear and non-local. This problem is believed to be well defined at all times for σ positive.

2.2.4 Other regularized Laplacian growth (rLG). These regularizations amount to introduce an UV cutoff δ in the physical space by evaluating $|f'_t|$ at a finite distance away from $\partial\mathbf{O}_t$. A possible choice [20] is $\rho_t(u)^{1/2} = \delta^{-1} \inf\{\varepsilon : \text{dist}[f_t(u + \varepsilon u); \partial\mathbf{O}_t] = \delta\}$. An estimation gives $\rho_t(u) \asymp |f'_t(u + \hat{\varepsilon}_u u)|^{-2}$ where $\hat{\varepsilon}_u$ goes to 0 with δ , so that it naively approaches $|f'_t(u)|^{-2}$ as $\delta \rightarrow 0$.

Another possible, but less physical, regularization consists in introducing an UV cutoff ν in the mathematical space so that $\rho_t(u) = |f'_t(u + \nu u)|^{-2}$.

2.2.5 Dielectric breakdown and generalizations. A larger class of problems generalizing Laplacian growth have been introduced. Their Loewner measures are as in Laplacian growth but with a different exponent:

$$\rho_t(u) = |f'_t(u)|^{-\alpha} \quad , \quad 0 \leq \alpha \leq 2.$$

Using an electrostatic interpretation of the harmonic potential, one usually refers to the case $\alpha = 1$ as a model of dielectric breakdown because the measure is then proportional to the local electric field $E_n = |f'_t(u)|^{-1}$. This is a phenomenological description. Just as the naive Laplacian growth these models are certainly ill-posed. They also require ultra-violet regularizations, one of which is described below using iterated conformal maps.

2.3 CUSP SINGULARITIES IN LG

The naive LG problem, without regularization, corresponds to the Loewner density $\rho_t(u) = |f'_t(u)|^{-2}$. The occurrence of singularities may be grasped by looking for the evolution of domains with a Z_n symmetry uniformized by the maps

$$f_t(w) = R_t w \left(1 + \frac{\beta_t}{n-1} w^{-n}\right)$$

for some $n > 2$ and with $|\beta_t| \leq 1$. This form of conformal maps is preserved by the dynamics. The conformal radius R_t and the coefficients β_t evolve with time according to $\partial_t R_t^2 = 2/(1 - \beta_t^2)$ and $\beta_t = (R_t/R_c)^{n-2}$ with R_c some integration constant. The singularity appears when β_t touches the unit circle which arises at a finite time t_c . At that time the conformal radius is R_c .

At t_c the boundary curve Γ_{t_c} has cusp singularities of the generic local form

$$\ell_c (\delta y)^2 \simeq (\delta x)^3$$

with ℓ_c a characteristic local length scale. In the present simple case $\ell_c \simeq R_c$. At time $t \nearrow t_c$, the dynamics is regular in the dimensionless parameter $\ell_c^{-1} \sqrt{t_c - t}$. The maximum curvature of the boundary curve scales as $\kappa_{\max} \simeq \ell_c / (t_c - t)$ near t_c and it is localized at a distance $\sqrt{t_c - t}$ away from the would be cusp tip. See Figure (1.17).

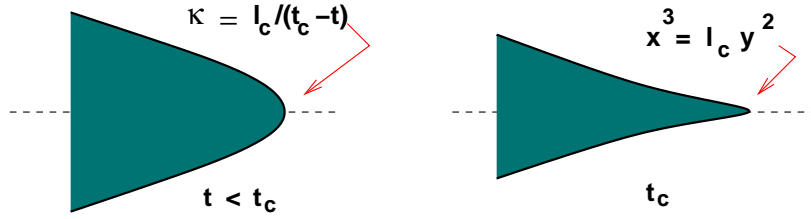


Figure 1.17 Cusp formation in Laplacian growth.

This behavior is quite generic. As we shall see, conformal maps $f_t(w)$ such that their derivatives are polynomials in w^{-1} are stable by the Laplacian growth dynamics. By construction, their zeroes are localized inside the unit disk. A singularity in the boundary curve occurs if one of these zeroes converges to the unit circle. The singularity is then a cusp $\ell_c y^2 \simeq x^3$ as can be seen by expanding locally the conformal map around its singular point.

Once regularized with an explicit ultraviolet cut-off, the processes are believed to be well defined for all time. The effect of the regularization procedure on the domain properties is presently unclear. The domain structures may a priori depend on how the problem has been regularized. In the hydrodynamic regularization –the Hele-Shaw problem– the cusp production is expected to be replaced by unlimited ramifications leading to dendritic growth.

In the regularized model, the curvature of Γ_t is expected to remain finite at all time. Using scaling theory, a crude estimate of its maximum around the would be singularities may be obtained by interchanging the short distance scale $\sqrt{t_c - t}$ near the singularity in the unregularized theory with the UV cutoff of the regularized theory. In the hydrodynamic regularization this gives $\kappa_{\max} \simeq \ell_c / \sigma^2$ as $\sigma \rightarrow 0$.

2.4 DISCRETE LOEWNER CHAINS

2.4.1 DLA. DLA stands for diffusion limited aggregation [15]. It refers to processes in which the domains grow by aggregating diffusing particles. Namely, one imagines building up a domain by clustering particles one by one. These particles are released from the point at infinity, or uniformly from a large circle around infinity, and diffuse as random walkers. They will eventually hit the domain and the first time this happens they stick to it. By convention, time is incremented by unity each time a particle is added to the domain. Thus at each time step the area of the domain is increased by the physical size of the particle. The position at which the particle is added depends on the probability for a random walker to visit the boundary for the first time at this position.

In a discrete approach one may imagine that the particles are tiny squares whose centers move on a square lattice whose edge lengths equal that of the particles, so that particles fill the lattice when they are glued together. The center of a particle moves as a random walker on the square lattice. The probability $Q(x)$ that a particle visits a given site x of the lattice satisfies the lattice version of the Laplace equation $\nabla^2 Q = 0$. It vanishes on the boundary of the domain, i.e. $Q = 0$ on the boundary, because the probability for a particle to visit a point of the lattice already occupied, i.e. a point of the growing cluster, is zero. The local speed at which the domain is growing is proportional to the probability for a site next to the interface but on the outer domain to be visited. This probability is proportional to the discrete normal gradient of Q , since the visiting probability vanishes on the interface. So the local speed is $v_n = (\nabla Q)_n$. It is not so easy to make an unbiased simulation of DLA on the lattice. One of the reasons is that on the lattice there is no such simple boundary as a circle, for which the hitting distribution from infinity is uniform. The hitting distribution on the boundary of a square is not such a simple function. Another reason is that despite the fact that the symmetric random walk is recurrent in 2d, each walk takes many steps to glue to the growing domain. The typical time to generate a single sample of reasonable size with an acceptable bias is comparable to the time it takes to make enough statistics on loop-erased random walks or percolation to get the scaling exponent with two significant digits. Still this is a modest time, but it is enough to reveal the intricacy of the patterns that are formed. Fig.1.18 is such a sample. The similarity with the sample in fig.1.1, obtained by iteration of conformal maps, is striking. But a quantitative comparison of the two models is well out of analytic control and belongs to the realm of extensive simulations.

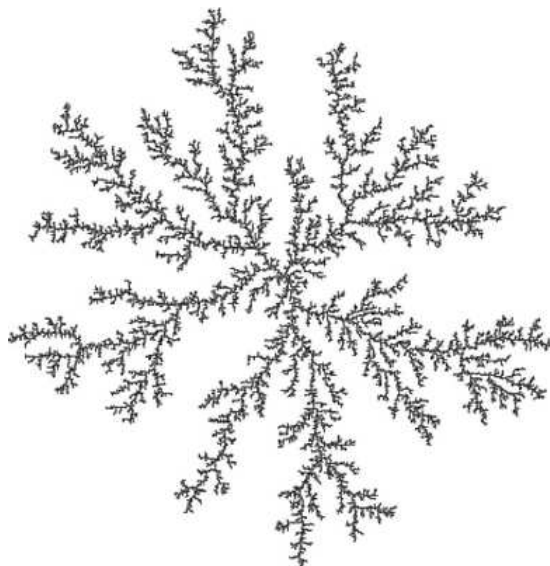


Figure 1.18 A DLA sample.

DLA provides a discrete analogue of Laplacian growth. The particle size plays the role of an ultraviolet cutoff. Since DLA only assumes that the growth is governed by the diffusion of elementary patterns, DLA has been applied to a large variety of aggregation or deposition phenomena, see eg.[18].

During this process the clustering domain gets ramified and develops branches and fjords of various scales. The probability for a particle to stick on the cluster is much higher on the tip of the branches than deep inside the fjords. This property, relevant at all scales, is responsible for the fractal structure of the DLA clusters.

Since its original presentation [15], DLA has been studied numerically quite extensively. There is now a consensus that the fractal dimension of 2d DLA clusters is $D_{\text{dla}} \simeq 1.71$. There is actually a debate on whether this dimension is geometry dependent but a recent study [19] seems to indicate that DLA clusters in a radial geometry and a channel geometry have identical fractal dimension. To add a new particle to the growing domain, a random walk has to wander around and the position at which it finally sticks is influenced by the whole domain. To rephrase this, for each new particle one has to solve the outer Laplace equation, a non-local problem, to know the sticking probability distribution. This is a

typical example when scale invariance is not expected to imply conformal invariance.

2.4.2 Iterated conformal maps. As proposed in [17], an alternative way to mimic the gluing of elementary particles consists in composing elementary conformal maps, each of which corresponds to adding an elementary particle to the domain.

One starts with an elementary map corresponding to the gluing of a tiny bump, of linear size λ , to the unit disk. A large variety of choices is possible, whose influence on the final structure of the domain is unclear. An example is given by the following formulæ (g_λ is the inverse map of f_λ):

$$\begin{aligned} g_\lambda(z) &= z \frac{z \cos \lambda - 1}{z - \cos \lambda} \\ f_\lambda(w) &= (2 \cos \lambda)^{-1} \left[w + 1 + \sqrt{w^2 - 2w \cos 2\lambda + 1} \right] \end{aligned}$$

where f_λ correspond to the deformation of the unit disk obtained by gluing a semi-disk centered at point 1 and whose two intersecting points with the unit circle define a cone of angle 2λ . For $\lambda \ll 1$, the area of the added bump is of order λ^2 . But other choices are possible and have been used.

Gluing a bump around point $e^{i\theta}$ on the unit circle is obtained by rotating these maps. The uniformizing maps are then

$$f_{\lambda;\theta}(w) = e^{i\theta} f_\lambda(w e^{-i\theta})$$

The growth of the domain is obtained by successively iterating the maps $f_{\lambda_n;\theta_n}$ with various values for the size λ_n and the position θ_n of the bumps. See Figure (1.19). Namely, if after n iterations the complement of the unit disk is uniformized into the complement of the domain by the map $F_{(n)}(w)$, then at the next $(n+1)^{\text{th}}$ iteration the uniformizing map is given by:

$$F_{(n+1)}(w) = F_{(n)}(f_{\lambda_{n+1};\theta_{n+1}}(w)) \quad (1.12)$$

For the inverse maps, this becomes $G_{(n+1)} = g_{\lambda_{n+1};\theta_{n+1}} \circ G_{(n)}$.

To fully define the model one has to specify the choice of the parameter λ_n and θ_n at each iteration. Since λ_n codes for the linear size of the added bump and since locally conformal maps act as dilatations, the usual choice is to rescale λ_{n+1} by a power of $|F'_{(n)}(e^{i\theta_n})|$ as:

$$\lambda_{n+1} = \lambda_0 |F'_{(n)}(e^{i\theta_n})|^{-\alpha/2}, \quad 0 \leq \alpha \leq 2$$

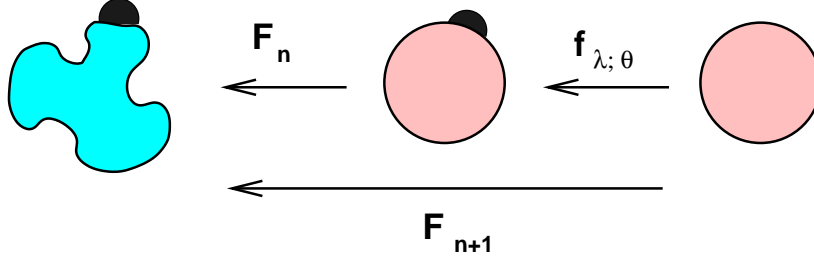


Figure 1.19 Iteration of conformal maps.

The case $\alpha = 2$ corresponds to DLA as the physical area of the added bump are approximatively constant and equal to λ_0 at each iterations. In the other case, the area of the added bump scales as $|F'_{(n)}(e^{i\theta_n})|^{2-\alpha}$.

The positions of the added bump are usually taken uniformly distributed on the mathematical unit circle with a measure $d\theta/2\pi$.

It is clear that this discrete model with $\alpha = 2$ provides a regularization of Laplacian growth with λ_0 playing the role of an ultraviolet cutoff. This may also be seen by looking at the *naive* limit of a small cutoff. Indeed, a naive expansion as $\lambda_n \ll 1$ gives that $F_{(n+1)} = F_{(n)} + \delta F_{(n)}$ with

$$\delta F_{(n)}(w) \simeq \lambda_n w F'_{(n)}(w) \left(\frac{w + e^{i\theta_n}}{w - e^{i\theta_n}} \right)$$

where we used the expression of f_λ for $\lambda \ll 1$. Using the recursive expression for λ_n and averaging over θ with a uniform distribution yields:

$$\langle \delta F(w) \rangle = \lambda_0 w F'(w) \oint \frac{d\theta}{2\pi} |F'(e^{i\theta})|^{-\alpha} \frac{w + e^{i\theta}}{w - e^{i\theta}}$$

For $\alpha = 2$ this reproduces the Loewner chain for Laplacian growth. But this computation is too naive as the small cutoff limit is not smooth, a fact which is at the origin of the non trivial fractal dimensions of the growing domains.

There are only very few mathematical results on these discrete models. The most recent one [27] deals with the simplest (yet interesting but not very physical) model with $\alpha = 0$. It proves the convergence of the iteration to well-defined random maps uniformizing domains of Hausdorff dimension 1. However, these models have been studied numerically extensively. There exists a huge literature on this subject but see ref.[24] for instance. These studies confirm that the fractal dimension of DLA clusters with $\alpha = 2$ is $D_{\text{dla}} \simeq 1.71$ but they also provide further informations on the harmonic measure multi-fractal spectrum. Results

on the α dependence of the fractal dimension may be found eg. in ref. [25].

Various generalizations have been introduced. For instance, in ref.[26] a model of iterated conformal maps has been defined in which particles are not added one by one but by layers. These models have one control parameter coding for the degree of coverage of the layer at each iterative step. By varying this parameter the model interpolates between discrete DLA and a discrete version of the Hele-Shaw problem. The fractal dimension of the resulting clusters varies with this parameter and seems to indicate that the fractal dimension of this discrete analogue of the Hele-Shaw problem is 2, a point that we shall discuss further in the last section.

2.5 INTEGRABILITY OF LAPLACIAN GROWTH

Laplacian growth is an integrable system, at least up to the cusp formation. Let us recall that it corresponds to a Loewner chain with a density $\rho_t(u) = |f_t(u)|^{-2}$, or equivalently to the quadratic equation

$$(\partial_\alpha \gamma_{t;\alpha}) (\partial_t \overline{\gamma_{t;\alpha}}) - (\partial_\alpha \overline{\gamma_{t;\alpha}}) (\partial_t \gamma_{t;\alpha}) = 2i \quad (1.13)$$

for the dynamics of the boundary points $\gamma_{t;\alpha} = f_t(u)$, $u = e^{i\alpha}$. What makes the model integrable is the fact that the r.h.s of eq.(1.13) is constant. Eq.(1.13) is then similar to a quadratic Hirota equation. Hints on the integrable structure were found in [21] and much further developed in [22, 23].

2.5.1 Conserved quantities. We now define an infinite set of quantities which are conserved in the naive unregularized LG problem. They reflect its integrability. We follow ref.[22, 23]. These quantities may be defined via a Riemann-Hilbert problem on Γ_t specified by,

$$S_+(\gamma) - S_-(\gamma) = \bar{\gamma} \quad , \quad \gamma \in \Gamma_t \quad (1.14)$$

for functions S_- and S_+ respectively analytic in the outer domain \mathbf{O}_t and in the inner domain \mathbf{K}_t . We fix normalization by demanding $S_-(\infty) = 0$. We assume Γ_t regular enough for this Riemann-Hilbert problem to be well defined. As usual, S_\pm may be presented as contour integrals:

$$S_\pm(z) = - \oint_{\Gamma_t} \frac{d\gamma}{2i\pi} \frac{\bar{\gamma}}{z - \gamma}.$$

The conserved quantities are going to be expressed in terms of S_\pm . We thus need their time evolution. Differentiation of eq.(1.14) with respect

to time and use of the evolution equation (1.13) gives:

$$\partial_t S_+(\gamma) - \partial_t S_-(\gamma) = 2g'_t(\gamma)/g_t(\gamma)$$

Notice now that $g'_t(\gamma)/g_t(\gamma)$ is the boundary value of $(\log g_t)'$ which by construction is analytic in \mathbf{O}_t . We may thus rewrite this equation as a trivial Riemann-Hilbert problem, $\partial_t S_+(\gamma) - (\partial_t S_- + 2(\log g_t)')(\gamma) = 0$, so that both terms vanish:

$$\partial_t S_+(z) = 0 \quad \text{and} \quad (\partial_t S_- + 2(\log g_t)')(z) = 0 \quad (1.15)$$

Since S_+ is analytic around the origin, we may expand it in power of z . Equation $\partial_t S_+(z) = 0$ then tells us that $S_+(z)$ is a generating function of conserved quantities: $S_+(z) = \sum_{k \geq 0} z^k I_k$ with

$$I_k = \oint_{\Gamma_t} \frac{d\gamma}{2i\pi} \bar{\gamma} \gamma^{-k-1}, \quad \partial_t I_k = 0. \quad (1.16)$$

This provides an infinite set of conserved quantities.

Since S_- is analytic around infinity, it may be expanded in power of $1/z$: $S_-(z) = -\mathcal{A}_t/\pi z + \dots$ with $\mathcal{A}_t = -\frac{i}{2} \oint_{\Gamma_t} d\gamma \bar{\gamma}$ the area of \mathbf{K}_t . The second equation $(\partial_t S_- + 2(\log g_t)')(z) = 0$ with $g_t(z) = R_t^{-1}z + O(1)$ then implies $\partial_t \mathcal{A}_t = 2\pi$. The area of the domain grows linearly with time, up to the time at which the first cusp singularity appears.

2.5.2 Simple solutions. A particularly simple class of conformal maps, solutions of the Laplacian growth equation, are those such that their derivatives are polynomials in w^{-1} . They may be expanded as:

$$f_t(w) = \sum_{n=0}^N f_n w^{1-n}, \quad f_0 = R_t > 0 \quad (1.17)$$

with N finite but arbitrary. The dynamical variables are the $N+1$ coefficient f_0, \dots, f_N . They are all complex except f_0 which is real. It will be convenient to define the function \bar{f}_t by $\bar{f}_t(w) = \overline{f_t(\bar{w})}$.

The fact that this class is stable under the dynamics follows from the Loewner equation (1.10). The trick consists in using the fact that the integration contour is on the unit circle so that $|f'_t(u)|^2 = f'_t(u) \bar{f}'_t(1/u)$. The contour integral then involves a meromorphic function of u so that it can be evaluated by deforming the contour to pick the residues. This is enough to prove that $\partial_t f_t(w)$ possesses the same structure as $f_t(w)$ itself so that the class of functions (1.17) is stable under the dynamics.

Alternatively one may expand the quadratic equation (1.13) to get a hierarchy of equations:

$$\sum_{n \geq 0} (1-n) [f_n \dot{\bar{f}}_{j+n} + \bar{f}_n \dot{f}_{-j+n}] = 2\delta_{j;0}$$

For $j = 0$, this equation tells us again that the area of the domain grows linearly with time. Besides this relation there are only N independent complex equations for $j = 1, \dots, N$ which actually code for the conserved quantities.

To really have an integrable system we need to have as many independent integrals of motion as dynamical variables. Thus we need to have N conserved quantities. These are given by the I_k 's defined above which may be rewritten as

$$I_k = \oint_{|u|=1} \frac{du}{2i\pi} \frac{f'_t(u) \bar{f}_t(1/u)}{f_t(u)^{k+1}}$$

Only the first N quantities, $I_0, \dots, I_{N-1} = R^{1-N} \bar{f}_N$ are non-vanishing. They are independent. They can be used to express algebraically all f_n 's, $n \geq 0$, in terms of the real parameter $f_0 = R_t$. The area law,

$$\mathcal{A}_t = \pi [R_t^2 + \sum_{n \geq 1} (1-n) |f_n|^2] = 2\pi t,$$

with the f_n 's expressed in terms of R_t , then reintroduces the time variable by giving its relation with the conformal radius.

2.5.3 Algebraic curves. As was pointed out in [23], solutions of Laplacian growth and their cusp formations have an elegant geometrical interpretation involving Riemann surfaces.

Recall that given a sufficiently smooth real curve Γ_t drawn on the complex plane one may define a function $S(z)$, called the Schwarz function, analytic in a ribbon enveloping the curve such that

$$S(\gamma) = \bar{\gamma}, \quad \gamma \in \Gamma_t$$

By construction, the Schwarz function may be expressed in terms of uniformizing maps of the domain bounded by the curves as $S(z) = \bar{f}_t(1/g_t(z))$.

The Riemann-Hilbert problem (1.14) defining the conserved charges then possesses a very simple interpretation: S_{\pm} are the polar part of the Schwarz function respectively analytic inside or outside Γ_t , i.e. $S(z) = S_+(z) - S_-(z)$. Thus the polar part S_+ , analytic in the inner domain, is conserved. The polar part S_- , analytic in the outer domain, evolves according to eqs.(1.15). Since $\log g_t(z)$ is analytic in the outer domain, these equations are equivalent to the single equation:

$$\partial_t S(z) = -2(\log g_t(z))' \quad (1.18)$$

Now the physical curve Γ_t may be viewed as a real slice of a complex curve, alias a Riemann surface. The latter is constructed using the

Schwarz function as follows. Recall that $s = S(z)$ is implicitly defined by the relations $z = f_t(w)$, $s = \bar{f}_t(1/w)$. In the case of polynomial uniformizing maps we get the pair of equations

$$\begin{aligned} z &= f_0 w + f_1 + f_2 w^{-1} + \cdots + f_N w^{1-N} \\ s &= \bar{f}_0 w^{-1} + \bar{f}_1 + \bar{f}_2 w + \cdots + \bar{f}_N w^{N-1} \end{aligned}$$

Eliminating w yields an algebraic equation for z and s only:

$$\mathbf{R}: \quad R(z, s) = 0 \tag{1.19}$$

with R a polynomial of degree N in both variables, $R(z, s) = \bar{f}_N z^N + f_N s^N + \cdots$. Eq.(1.19) defines an algebraic curve \mathbf{R} . It is of genus zero since by construction it is uniformized by points w of the complex sphere. It has many singularities which have to be resolved to recover a smooth complex manifold.

The Riemann surface \mathbf{R} may be viewed as a N -sheeted covering of the complex z plane: each sheet corresponds to a determination of s above point z . At infinity, the physical sheet corresponds to $z \simeq f_0 w$ with $w \rightarrow \infty$ so that $s \simeq (z/f_0)^{N-1} \bar{f}_N$, the other $N-1$ sheets are ramified and correspond to $z \simeq f_N/w^{N-1}$ and $s \simeq \bar{f}_0/w$ with $w \rightarrow 0$ so that $z \simeq (s/\bar{f}_0)^{N-1} f_N$. Hence infinity is a branch point of order $N-1$.

By the Riemann-Hurwitz formula the genus g is $2g-2 = -2N + \nu$ with ν the branching index of the covering. Since the point at infinity counts for $\nu_\infty = N-2$, there should be N other branch points generically of order two. By definition they are determined by solving the equations $R(z, s) = 0$ and $\partial_s R(z, s) = 0$. Since the curve is uniformized by $w \in \mathbf{C}$, these two equations imply that $z'(w) \partial_z R(z(w), s(w)) = 0$. Hence either $z'(w) = 0$, $\partial_z R \neq 0$, and the point is a branch point, or $z'(w) \neq 0$, $\partial_z R = 0 = \partial_s R$, and the point is actually a singular point which needs to be desingularized. So the N branch points at finite distance are the critical points of the uniformizing map $z = f_t(w)$.

The curve \mathbf{R} possesses an involution $(z, s) \rightarrow (\bar{s}, \bar{z})$ since $R(\bar{s}, \bar{z}) = \overline{R(z, s)}$ by construction. The set of points fixed by this involution has two components: (i) a continuous one parametrized by points $w = u$, $|u| = 1$ —this is the real curve Γ_t that we started with— and (ii) a set of N isolated points which are actually singular points.

The cusp singularity of the real curve Γ_t arises when a isolated real point merges with the continuous real slice Γ_t . Locally the behavior is as for the curve $u^2 = \varepsilon v^2 + v^3$ with $\varepsilon \rightarrow 0$.

The simplest example is for $N = 3$ with \mathbf{Z}_3 symmetry so that $f_t(w) = w + b/w^2$ and

$$w^2 z = w^3 + b \quad , \quad w s = 1 + b w^3$$

We set $f_0 = 1$ and $f_3 = b$. Without loss of generality we assume b real. The algebraic curve is then

$$R(z, s) \equiv bz^3 + bs^3 - b^2s^2z^2 + (b^2 - 1)(2b^2 + 1)sz - (b^2 - 1)^3 = 0$$

Infinity is a branch point of order two. The three other branch points are at $z = 3\omega(b/4)^{1/3}$, $s = \omega^2(2b^2 + 1)(2b)^{-1/3}$ corresponding to $w = \omega(2b)^{1/3}$ with ω a third root of unity. They are critical points of $z(w)$. There are three singular points at $z = \omega(1 - b^2)/b$, $s = \omega^2(1 - b^2)/b$ corresponding to $w = \omega(1 \pm \sqrt{1 - 4b^2})/2b$. The physical regime is for $b < 1/2$ in which case the real slice $\Gamma_t = \{z(u), |u| = 1\}$ is a simple curve. The singular points are then in the outer domain and the branch points in the inner domain. The cusp singularities arise for $b = 1/2$. For $b > 1/2$ there are no isolated singular points, they are all localized on the real slice so that Γ_t possesses double points. See Figure (1.20).

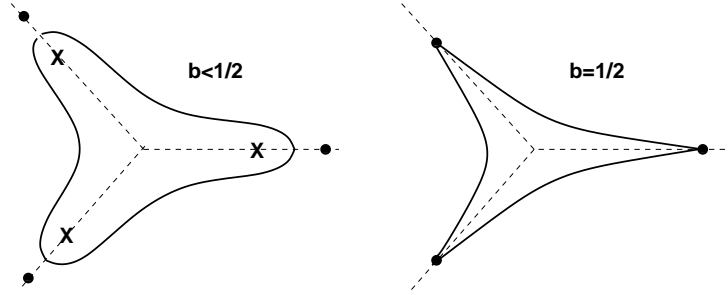


Figure 1.20 Subcritical and critical algebraic curves. Black circles are singular points. Crosses are branch points.

2.6 DENDRITIC ANOMALIES

We now would like to discuss a few points concerning the regularized models and their small cut-off limits –which are actually what we are interested in. We shall point out that the hydrodynamic regularization used in the Hele-Shaw problem possesses essential differences with that used in other regularized models, say DLA. This opens the possibility for the Hele-Shaw problem and DLA not to be in the same universality class.

This observation is based on the conjectural existence of anomalies in the Hele-Shaw problem –a word which refers to quantities which, although naively vanishing in the small cut-off limit, are actually non zero but finite in this limit due to compensating effects.

An analogy with Burgers turbulence may be useful. The 1d Burgers equation is $\partial_t u + u \partial_x u - \nu \partial_x^2 u = 0$ for a velocity field $u(t, x)$. The viscosity ν plays the role of ultraviolet cut-off. At $\nu = 0$ this equation is simply Euler equation which may be easily solved. At $\nu = 0$, any smooth initial data produces shocks in finite time with a discontinuity of u . In the regularized equation with $\nu \neq 0$, there is no shock production but the field $\hat{\epsilon} \equiv \nu(\partial_x u)^2$, which naively vanishes when $\nu \rightarrow 0$, has actually a non trivial limit. It does not vanish because there is a compensation between small viscosity ν and large velocity gradient $(\partial_x u)$. The field $\hat{\epsilon}$ codes for the amount of energy dissipated inside the shocks.

The analogy that we would like to put forward is that the cusp formation in Laplacian growth is analogous to shock formation in Burgers and that the surface tension σ in Laplacian growth plays the role of the viscosity in Burgers. There are potential compensating effects between small surface tension and large curvature in the Hele-Shaw problem.

2.6.1 Almost conserved quantities. We now describe the effect of the regularization procedure on the conserved quantities of Laplacian growth. Recall that they were defined starting from the Riemann-Hilbert problem:

$$h_+(\gamma) - h_-(\gamma) = \bar{\gamma} \quad , \quad \gamma \in \Gamma_t \quad (1.20)$$

for functions h_- and h_+ respectively analytic in \mathbf{O}_t and \mathbf{K}_t . We use the notation h_{\pm} instead of S_{\pm} in order to avoid confusion with the unregularized Laplacian growth. We again fix normalization by demanding $h_-(\infty) = 0$ so that $h_{\pm}(z) = -\oint_{\Gamma_t} \frac{d\gamma}{2i\pi} \frac{\bar{\gamma}}{z-\gamma}$. Time differentiating eq.(1.20) using the evolution equation (1.9) now gives:

$$\partial_t h_+(\gamma) - \partial_t h_-(\gamma) = 2 \frac{g'_t(\gamma)}{g_t(\gamma)} \frac{v_n(\gamma)}{|g'_t(\gamma)|} \quad (1.21)$$

with v_n the boundary normal velocity –in LG, we had $v_n = |g'_t(\gamma)|$.

In the case of the Hele-Shaw (HS) problem, the hydrodynamic regularization of Laplacian growth, the normal velocity possesses a particular form (1.11) involving the derivative of ϑ . Eq.(1.21) may then be rewritten in terms of the potential, $\Phi_t(z) = \log g_t(z) + \sigma \vartheta_t(g_t(z))$, and of the curvature as:

$$\partial_t h_+(\gamma) - \partial_t h_-(\gamma) = 2\Phi'_t(\gamma) - 2\sigma\kappa'_t(\gamma)$$

Since Φ_t is analytic in \mathbf{O}_t , the solution of this equation is given by that of the Riemann-Hilbert problem for κ_t . So, let κ_- and κ_+ be respectively

analytic in \mathbf{O}_t and \mathbf{K}_t with boundary values $\kappa_+ - \kappa_- = \kappa_t$ on Γ_t . Then:

$$\begin{aligned}\partial_t h_+(z) &= -2\sigma \partial_z \kappa_+(z) \\ \partial_t h_-(z) &= -2\partial_z \Phi_t(z) - 2\sigma \partial_z \kappa_-(z)\end{aligned}\tag{1.22}$$

These equations codes for the behavior of h_{\pm} in the limit of vanishing surface tension.

A noticeable point is that the above r.h.s. are total derivatives. In particular, contribution to the $1/z$ term in $\partial_t h_-$ only comes from the logarithmic factor in the potential. This implies that at $\sigma \neq 0$ the area of the domains also grows linearly with time, $\mathcal{A}_t \simeq 2\pi t$ at large time³, and it is independent of the UV cutoff σ . This is contrast with other regularizations for which the area growth may be cutoff dependent.

2.6.2 A conjecture. The supplementary terms proportional to $\sigma \kappa'_{\pm}$ in the quasi conservation laws (1.22) naively vanish when the UV cutoff is removed. *Dendritic anomalies* refer to the possibilities for these terms not to vanish as the cutoff goes to zero, say $\sigma \rightarrow 0$ in the Hele-Shaw (HS) problem. Such possibility arises due to a balance between small surface tension and large curvature.

Recall the previous HS estimation of the maximum curvature $\kappa_{\max} \simeq \ell_c / \sigma^2$ with ℓ_c the local scale associated to the cusp. These maxima are localized around points γ_c which would turn into cusp singularities in absence of surface tension. So, we may expect that in the HS problem the product $\sigma \kappa(\gamma)$ is a function picked around its maximum values and is of the form $\frac{\ell_c}{\sigma} \varphi(\frac{\gamma - \gamma_c}{\sigma})$ when the point γ moves away from γ_c with φ finite at the origin and decreasing rapidly away from it. For isolated singular points γ_c , this would converge in the limit $\sigma \rightarrow 0$ to a sum of Dirac point measures.

This leads us to conjecture that the anomalous term $\sigma \kappa(\gamma)$ goes to a non trivial but finite distribution as $\sigma \rightarrow 0$. This distribution then contributes to eq.(1.22) to break the ‘classical’ conservation laws valid in the unregularized theory, hence the name *dendritic anomaly*.

The Loewner equation (1.7) –or the evolution equation (1.9)– are then expected to have a finite limit as $\sigma \rightarrow 0$ with a non trivial right hand side. The solution would be well-defined for all times and would describe a non trivial family $\tilde{\mathbf{K}}_t$ such that, for fixed t , $\tilde{\mathbf{K}}_t$ is the limit of the domains \mathbf{K}_t as $\sigma \rightarrow 0$. This is consistent with the observation that the area of \mathbf{K}_t is independant of σ and grows linearly with time for any

³This result concerning the area is simply a consequence of the fluid incompressibility. But the general method allows to deal with the complete hierarchy of quasi conserved charges.

σ , ie. $\mathcal{A}_t \simeq 2\pi t$, so that the existence of a limiting set $\hat{\mathbf{K}}_t$ is not ruled out.

It is implicit in the previous conjecture that the uniformizing maps f_t have a finite limit, say \hat{f}_t , as $\sigma \rightarrow 0$ such that the image of the unit circle by \hat{f}_t is the boundary of $\mathbf{C} \setminus \hat{\mathbf{K}}_t$. This leads us to conjecture that the limiting domain $\hat{\mathbf{O}}_t$, which is the component of $\mathbf{C} \setminus \hat{\mathbf{K}}_t$ containing infinity, is uniformized onto \mathbf{D} by $\hat{g}_t \equiv \hat{f}_t^{-1}$.

Let R_t be the conformal radius computed at finite σ using the maps f_t . Recall that if D_{hs} is the fractal dimension we have $R_t^{D_{\text{hs}}} \asymp \mathcal{A}_t$ for large t . By dimensional analysis $R_t \simeq \sigma(\mathcal{A}_t/\sigma^2)^{1/D_{\text{hs}}}$ since σ has dimension of a [length]. Because in the HS problem the area grows linearly with time without any dependence on σ , this also reads:

$$R_t^{D_{\text{hs}}} \simeq \sigma^{D_{\text{hs}}-2} t$$

Since we expect the limiting domains and the limiting conformal maps to exit, R_t should have a finite limit as $\sigma \rightarrow 0$ which coincides with the conformal radius \hat{R}_t computed using \hat{f}_t . As consequence, we expect:

$$D_{\text{hs}} = 2$$

That is: the fractal dimension of Laplacian growth clusters, within the hydrodynamic regularization, is 2. If these conjectures are true, they imply that the Hele-Shaw problem is not in the same universality class as DLA.

These conjectures are compatible with that of ref.[26] based on numerical studies of generalized iterated conformal maps. They are not expected to apply to arbitrary regularizations because in these cases the area may depend on the UV cutoff and the previous dimensional analysis does not apply. It would then be natural to wonder whether we may define renormalized uniformizing maps in the limit of a vanishing cutoff.

Acknowledgments

It is a pleasure thank Vincent Pasquier and Paul Wiegmann for discussions on this problem and the organizers of the Cargèse 2004 ASI for providing us the opportunity to write these notes.

Work supported in part by EC contract number HPRN-CT-2002-00325 of the EUCLID research training network.

References

- [1] A. Belavin, A. Polyakov, A. Zamolodchikov, *Infinite conformal symmetry in two-dimensional quantum field theory*, Nucl. Phys. **B241**, 333–380, (1984).
- [2] J. Cardy, J. Phys. **A25** (1992) L201–206.
The rigorous proof is in
S. Smirnov, C.R. Acad. Sci. Paris **333** (2001) 239–244.
- [3] G. Watts, J. Phys **A29** (1996) L363–368.
The rigorous proof is in
J. Dubédat, *Excursion Decompositions for SLE and Watts’ crossing formula*, preprint, arXiv: math.PR/0405074
- [4] O. Schramm, Israel J. Math., **118**, 221–288, (2000);
- [5] G. Lawler, O. Schramm and W. Werner, (I): Acta Mathematica **187** (2001) 237–273; arXiv:math.PR/9911084
G. Lawler, O. Schramm and W. Werner, (II): Acta Mathematica **187** (2001) 275–308; arXiv:math.PR/0003156
G. Lawler, O. Schramm and W. Werner, (III): Ann. Henri Poincaré **38** (2002) 109–123. arXiv:math.PR/0005294.
- [6] S. Rohde and O. Schramm, arXiv:math.PR/0106036; and references therein.
- [7] V. Beffara, *The dimension of the SLE curves*, arXiv: math.PR/0211322.
- [8] J. Dubédat, *SLE(κ, ρ) martingales and duality*, to appear in Ann. Probab. arXiv:math.PR/0303128
- [9] G. Lawler, introductory texts, including the draft of a book, may be found at <http://www.math.cornell.edu/~lawler>
W. Werner, *Lectures notes of the 2002 Saint Flour summer school*
- [10] M. Bauer and D. Bernard, Commun. Math. Phys. **239** (2003) 493–521, arXiv:hep-th/0210015, and Phys. Lett. **B543** (2002) 135–138;
M. Bauer and D. Bernard, Phys. Lett. **B557** (2003) 309–316, arXiv:hep-th/0301064;
M. Bauer and D. Bernard, Ann. Henri Poincaré **5** (2004) 289–326, arXiv:math-ph/0305061.
M. Bauer and D. Bernard, *SLE, CFT and zig-zag probabilities*, arXiv:math-ph/0401019.
M. Bauer, D. Bernard and J. Houdayer, *Dipolar SLEs*, arXiv:math-ph/0411038
- [11] R. Friedrich and W. Werner, *Conformal restriction, highest weight representations and SLE*, arXiv:math-ph/0301018.
- [12] , B. Duplantier *Conformal Fractal Geometry and Boundary Quantum Gravity*, arXiv:math-ph/0303034.

- [13] John B. Conway, *Functions of One Complex Variable II*, Springer-Verlag, New York, New York, 1995
- [14] D. Bensimon, L. Kadanoff, S. Liang, B. Shraiman, C. Tang, Rev. Mod. Phys. **58** (1986) 977, and references therein.
- [15] T. Witten and L. Sander, Phys. Rev. Lett. **47** (1981) 1400.
- [16] L. Niemeyer, L. Pietronero and H. Wiesmann, Phys. Rev. Lett. **52** (1984) 1033.
- [17] M. Hasting and S. Levitov, Physica **D116** (1998) 244.
- [18] T. Hasley, Physics Today, **53**, Nov. 2000, 36-41;
M. Bazant, D. Crowdy, *Conformal methods for interfacial dynamics*, arXiv:cond-mat/0409439, and references therein.
- [19] E. Somfai, R. Ball, J. deVita, L. Sander, ArXiv:cond-mat/0304458.
- [20] L. Carleson and N. Makarov, Commun. Math. Phys. **216** (2001) 583.
- [21] B. Shraiman, D. Bensimon, Phys. Rev A **30** (1984) 2840.
- [22] S. Richardson, Euro. J. of Appl. Math. **12** (2001) 571.
- [23] I. Krichever, M. Mineev-Weinstein, P. Wiegmann and A. Zabrodin, arXiv:nlin.SI/0311005, and refs. therein.
- [24] B. Davidovitch, H. Hentschel, Z. Olami, I. Procaccia, L. Sander, E. Somfai, Phys. Rev. **E59** (1999) 1368.
M. Jensen, A. Levermann, J. Mathiesen, I. Procaccia, Phys. Rev. **E65** (2002) 046109.
- [25] M. Hastings, arXiv:cond-mat/0103312.
- [26] H. Hentschel, A. Levermann, I. Procaccia, arXiv:cond-mat/0111567.
- [27] S. Rohde, M. Zinsmeister, *Some remarks on Laplacian growth*, preprint April 2004.